ADDIS ABABA UNIVERSITY

COLLEGE OF NATURAL AND COMPUTATIONAL SCIENCES

SCHOOL OF EARTH SCIENCES

"APPLICATION OF GEOPHYSICAL METHODS FOR DELINATING DEEP AND SHALLOW GROUND WATER FLOW SYSTEMS ALONG ZIWAY-BUTAJIRA AND MEKI-MIDREKEBD TRAVERSES, CENTRAL MER, AND THEIR IMPLICATION FOR FLUORIDE CONCENTRATION"

A Thesis Submitted to

School of Graduate Studies

Department of Earth Science

By

Mandefro Ararso

Addis Ababa
May, 2017

APPLICATION OF GEOPHYSICAL METHOD FOR DELINATIG SHALLOW AND DEEP GROUND WATER FLOW SYSTEM ALONG ZIWAY-BUTAJIRA AND MEKI-MIDREKEBD TRAVERSES, CENTRAL MER, AND THIER IMPLICATION FOR FLOURIDE CONCENTRATION

A THESIS SUBMITTED TO THE SCHOOL OF GRADUATE STUDIES ADDIS ABABA UNIVERSITY IN PARTIAL FULFILLMENT OF THE REQUIREMENT FOR THE DEGREE OF MASTER OF SCIENCE IN APPLIED GEOPHYSICS

ADDIS ABEBA UNIVERSITY

SCHOOL OF GRADUATES STUDIES

DEPARTEMENT OF EARTH SCIENCE

BY

MANDEFRO ARARSO

MAY, 2017 (2009 E.C)

ADDIS ABEBA UNIVERSITY

SCHOOL OF GRADUATES STUDIES

DEPARTEMENT OF EARTH SCIENCE

APPLICATION OF GEOPHYSICAL METHOD FOR DELINATING SHALLOW AND DEEP GROUND WATER FLOW SYSTEM ALONG ZIWAY-BUTAJIRA AND MEKI-MIDREKEBD TRAVERSES, CENTRAL MER, AND SHOW THERE IMPLICATION FOR FLOURIDE CONCENTRATION

BY

MANDEFRO ARARSO
COLLEGE OF NATURAL AND COMPUTIONAL SCIENCES
DEPARTEMENT OF EARTH SCENCE

APPROVED BY BOARD OF EXAMINER:

Dr. Mulugeta Alene Signature ___________.

Chairman School Graduate Committee

Prof. Tigistu Haile Signature____________.

Advisor

_______________________ Signature___________.

External Examiner

_______________________ Signature________.

Internal Examiner

Acknowledgement

First of all, I would to thank the almighty God for everything He does in my life.

I have got no words to express my advisor Prof. Tigistu Haile for his crucial comment and sound suggestion that he gave me in order to accomplish this thesis successfully. During the time that I engaged in this thesis work, he acted like not only my advisor but also like my father and colleague. I thank you for everything that you did for me.

I great fully thanks to Dr. Bekele Abebe for his fatherly approach, encouragement, positive comment especially during my field work.

I would like to greatly thank my classmate Mekdes Samuel for her support in the field work and data collection phase of the work.

I would like to very greatly thank the EU funded FLOWERED Project for engaging me in the work it is conducting along the Ziway-Butajira and Meki-MidreKebd areas to investigate the geophysical signatures for the possible causes for variation in fluoride concentration along these sectors, specifically along the Rift Floor-Western Escarpment traverses, and for their financial support for my research work

My gratitude also goes to the Geomatrx PLC, a member of the FLOWERED Project, specifically Ato Kifle for assisting me in collecting the MT data and sharing me their knowledge,experience and their assistance on the MT computer software. My gratitude also goes to waterworks design and supervision enterprise (WWDSE) for providing me all the necessary additional secondary data.

Last but not least, my deepest heartfelt gratitude goes to my beloved wife and family, Meselch Kassa, Kaleab Mandefro and Elieni Mandefro who were my source of inspiration. Their love and encouragement have played important role throughout my academic life.

ABSTRACT

An integrated geophysical survey using Vertical Electrical Sounding (VES) and Audio Magneto Telluric (AMT) method was conducted to separate shallow and deep ground water flow systems and the role geological structure play in the movement of these waters from Rift Floor to Western Escarpment sectors, specifically through geophysical work along the Ziway-Butajira and Meki-MidreKebd traverses. These methods were selected for their resolution and ability to map the shallow to intermediate depth (VES) and the deeper (AMT) horizons in the subsurface.

Geographically the Ziway-Butajira and Meki- Midrekebd areas lie in the Central Main Ethiopian Rift within Oromia and South Nations, Nationalities and Peoples Regional State in Ethiopia. The areas also lie on dominantly volcanic and lacustrine deposit terrain. The geophysical survey included twenty three (23) VES point using Schlumberger array with maximum half current electrodes AB/2 =750m and twenty seven (27) 2DAMT measuring points. These data were interpreted both qualitatively and quantitatively in order to infer the subsurface geoelectrical stratification of the area and hence the geology as well as the major geologic structures over the transects. It was also possible to extract information on the presence of groundwater bearing horizons in the subsurface including their location and depth.

The qualitative analysis of VES data were performed by using apparent resistivity psuedodepth sections constructed for VES points oriented in a near collinear direction, while the qualitative interpretation of the 2D AMT data were also performed by using 2D MT geoelectric sections. For quantitative interpretation, the individual VES data were interpreted using the ResixIP and Win Resist modeling software to obtain the layer parameters beneath each VES and constructing the geoelectrical sections along selected survey lines. The interpretation of the VES during modeling was constrained by lithological logs from two nearby boreholes. The information from VES data and the borehole were also used to constrain the depth information in the 2D MT modeling which are conducted on four survey line.

In general, the VES result revealed four to five main geoelectrical layers that differ in degree of weathering and fracturing, composition and depth of burial. The geoelctrical sections further enabled the identification of the depth to the aquifer along the survey line. On the other hand, the 2D AMT help to identify low resistivity zones and structures that extend to larger depth- which has easily mapped the subsurface to depths of about 1200 m. Finally the overall interpretation was done by integrating all the above result together with the topographic maps and bore hall information. As a result of these shallow and deep ground water systems and geological structures are identified. It is found that vertical and near vertical structures that extend to larger depth is mapped along the traverses showing that there is a flow of shallow groundwaters to the deeper horizons, with no major separation between the two groundwater systems. It has also been possible to delineate drilling sites for potential productive boreholes.

Table of Contents

List of Figures

List of Tables

CHAPTER ONE

INTRODUCTION

1.1 Background

The Ethiopian Rift is part of the East African Rift System (EARS), which is the one of the largest sub-aerial tectonic phenomenon of the world, where the Earth's tectonic forces are currently trying to split up the old African plate into Nubian (African) and Somalia plates. In the Ethiopian section, this huge volcano tectonic sunken block stretches for nearly 1000 km in a NE-SW direction connecting the Kenyan Rift to south and the Red Sea and Gulf of Aden Rifts to the north with an average width of 70 km (Mohr, 1971;; Boccaletti et al, 1999; Abebe et al., 2007). The rift forms a contradicting landscape ranging from wide faulted plains of the valley floor lying 120 m.b.s.l. in the Afar Depression, where the Ethiopian, Red Sea and Gulf of Aden Rift radiate to the uplifted adjacent plateaus, rising to 2,000–3,500 a.m.s.l. The Ethiopian Rift can be divided into two major physiographic sections: the Main Ethiopian Rift (MER) and the Afar Depression. The MER represents the northernmost active segment of the EARS, connecting the rift system with the Afar Depression (Abebe et al., 2007). The rift system is characterized by a complex pattern of narrow belts of parallel faults and sunken strips of land between two faults giving rise to a rift in rift structure.

Rifting was accompanied by widespread volcanic and sedimentation processes since Oligocene Miocene (Kazmin et al., 1978; Gidey Wolde Gabriel et al., 1990). As land dissection and spreading continued in response to tensional forces, extensive episodic volcanic eruptions took place accompanied by series of faulting (Abebe et al., 2005). The volcanic rocks are dominantly fissure basaltic lava flows, rhyolites and ignimbrites associated with volcano-classic tuff and ash deposits. The basalt extrusions were interspersed with large accumulations of rhyolite and trachyte, breccia, ignimbrite and shallow basic intrusions (Kazmin, 1979). In the rift floor continental type volcanism has developed, giving rise to large Salic rocks from central type eruptions accompanied by fissure basic lava flows in places covered by thick lacustrine and alluvia colluvium quaternary deposits. Volcanism has persisted into the present time in the Afar region within small eruptive centers. In general, the shape of the Ethiopian Rift today is the results of different geological processes such as uplift, doming and eventual rupturing and volcanism.

Ethiopian rift consists of three major regions with distinct volcanic and tectonic characteristics representing different stages of rifting. These are the broadly rifted zone of south-western Ethiopia, the Main Ethiopian Rift (MER) of central Ethiopia, and the Afar Depression. The study area, which is known by the name Ziway –butajira and meki traverse, is located at the center of the MER some 200 km south of the capital Addis Ababa. The MER is characterized by a complex nested natural lakes fed by rivers and groundwater that originate from eastern and western highlands. Four major lakes occupy ancestral depressions of Plio-Pleistocene calderas at the center of the basin. The lakes vary significantly in size, depth, hydrochemistry and hydro geological setting.

The presence of many lakes and geothermal fields within a complex rift attracted major geoscientific and limn logical investigations since the second half of the 20th century. Many of the geoscientific investigations related to hydrogeology and hydrochemistry revealed the importance of water–rock interactions in influencing the water quality in different parts of the Ethiopian rift and adjacent escarpments (Teklehaimanot et al., 1987; Tesfaye Chernet et al., 2001). Very few studies provided information on how groundwater quality is influenced along flow paths at regional scale all the way from the Ethiopian highlands to the rift (Tenalem Ayenew, 2005; Seifu Kebede et al., 2005). Some studies revealed temporal changes of the quality of the lakes caused by anthropogenic influences (Tenalem Ayenew and Dagnachew Legesse, 2007).

Programs have been initiated over the last few decades, but groundwater provision is often unsuccessful Water well drilling because of poor water quality and productivity. This problem is exacerbated by lack of understanding of the groundwater flow system. Information on groundwater circulation and hydro chemical evolution is poorly understood, except few general studies made at sub-regional scale (Tesfaye Chernet et al., 2001; Tenalem Ayenew, 2003). Groundwater circulation patterns, recharge source and interactions between lakes and groundwaters have also been the subject of few studies in the southern MER (McKenzie et al., 2001).In Ethiopia, well water, spring water The volcanic rocks, particularly in the young basalt, contain high concentrations of fluoride and Fluor apatite. Large fault systems in the Valley create conditions that allow very deep percolation of infiltrating surface water. The floor of the Rift Valley that is characterized by high hydrothermal activity accelerates the solubility of fluoride. The hot climate and high fluoride waterbed of the Rift Valley, therefore, favor the development of endemic fluorosis. The water supplies in the Ethiopian Rift Valley region come mainly from boreholes with depths from 10 to 100 meters and Tap water are the common water supply source used in both urban and rural areas. The amount of fluoride present naturally in non-fluoridated drinking water is highly variable, being dependent upon the individual geological environment from which the water is obtained. However, water is epidemiologically most essential sources of fluoride in most areas, considerable exposure risk is also associated with the consumption of fish bones, canned meat, vegetables, grains and other staples, local salt, drinks (especially tea) and air (WHO, 1984). Contrarily, in some African and Asian communities, intake of fluoride from food has been found to be higher than from water.

Fluoride in drinking water could be beneficial or detrimental health depending on its concentration, and total amount ingested. The important effects on human are growth being incorporated in to the mineral part of bones and in teeth in the form of Fluor apatite at low concentrations. On the other hand, excessive exposure to fluoride can causes for dental and skeletal fluorosis. Several studies, during the last 5-6 years, revealed that life-long impact and accumulation of fluorides causes not only human skeletal and teeth damage, but also changes in the DNA-structure, paralysis of volition, cancer, etc. In summary, this study is believed to give some initial information for the future detailed study in the area and as such basically the aim of this work is to locate the shallow and deep ground water flow systems in the study area and also to show their implication for fluoride concentration. It is as well designed to map structures (such as fault, dykes and weak zones) and also define the vertical electrical/geological stratification of the study area by using geophysical integrated method sand their role in the groundwater flow system.

1.2 Statement of the Problem

The two traverses selected for this work, i.e. the Ziway-Butajita and Meki-MidreKebd lines traverse the rift floor to western rift escarpment areas and show clear variation in fluoride concentration of the waters .The traverses are situated in both the Oromia and Southern Nations and Nationality Regional State (SNNPRS), as it is seen from the Figure (1.1) which are characterized by both excessive exposure to fluoride and by the scarcity of both subsurface and surface water. Therefore, a detailed study to illustrate the subsurface groundwater flow systems, which may have influence of the groundwater pollution, is indispensable in this area. The exploration of groundwater done so far is not adequate to solve the problem in relation to this pollution and the demand for clean water raised in the society. This study is hence intended to solve this problem in the specific locations by developing the geoelectrical section of the subsurface, through which the shallow and deep ground water flow systems and there implication on fluoride concentration can be extracted from.

1.3 Location and Accessibility

Ziway -Butajira and Meki- MidreKebd traverse is found both in the SNNPRS and in Oromai Region of the Main Ethiopian Rift (Figure 1.1).The study area extends from Butjira (in the North West) to Ziway (in the south east); and from Meki (in the north east) to Midrer Kebd in the North. The area is accessible by two routes from Addis Ababa. One route is the asphalt road that runs from Addis Ababa-Majo-Ziway with a distance of 163 km; and another route is Addis Ababa Alem Gena-Butajira asphalt road with a distance of 133km and Butajira-Ziwayall-weather road segment having a distance of about 60 km The Ziway -Butajira traverse represents the rift floor portion of the basin. Most of the study area covers the low lying plain land that runs from Meki, and some portion of it touches the lower part.

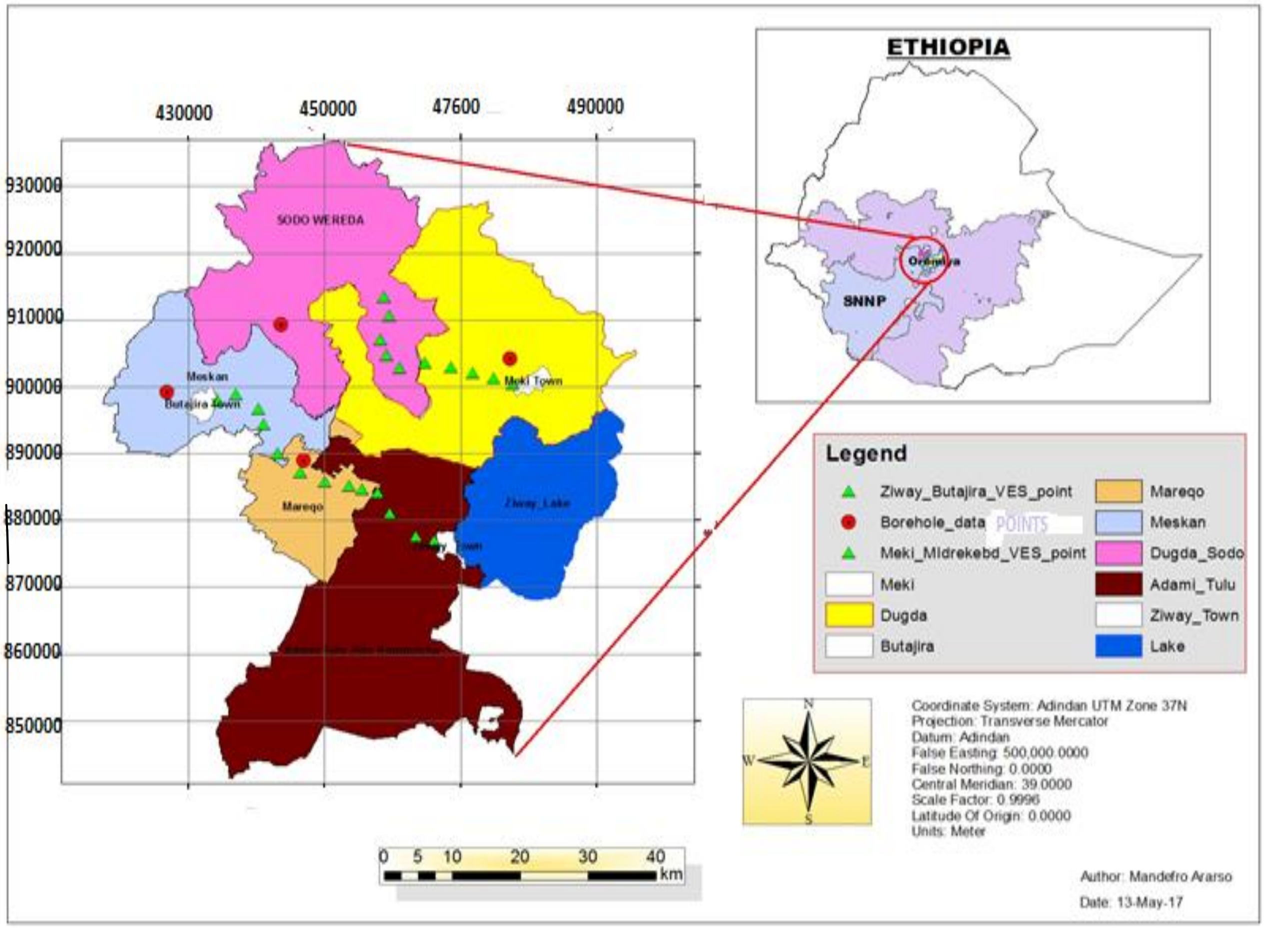

Figure 1.1 Location map of the study showing the different Woredas. The location of the VES points (triangles)

And bore holes in the area (circles) are also indicated

1.4 Objectives of the Study

1.4.1 General Objective

To understand the general subsurface electrical stratification and geologic structures of the area so as to delinate the deep and shallow ground water flow systems and show their possible implication on the fluoride concentration.

1.4.2 Specific objectives

- Defining the vertical geological stratification of the area along the traverses with a view to determine the existence of water bearing horizons and their depth,
- Mapping subsurface structures along the traverses that may control the flow of subsurface water from Rift escarpment to the Rift floor,
- To extract information on water quality and show its relationship with shallow and deep ground water flow systems,

1.5. Previous Works

A number of studies have been carried out in Central Ethiopia Rift Valley that includes the study area .These studies have been focusing on the geology, volcano tectonic, hydrogeological, hydrology, groundwater flow direction and water resources potential assessment of the areas which directly or indirectly are related to the current study some of the works are briefly described as follows:

1/Hydrogeology and underground water modeling (Ministry of Water Resources and Water Technology Center, 2008)

These studies report delineated the aquifer and aquifer properties of the study area, the study area based on geomorphologic features were classified in to the western escarpment, butajira crescent, cinder cone and basaltic area.

Ministry of water research based on the geological, geophysical survey, test drilling result and applying additional field investigation, the hydro geological characteristics of the study are had been explained as follow.

- Lake Ziway is connected to the ground water the lake receive ground water from the eastern and its north east side and ground water output from the lake takes place at its south western side.
- The ground water in pyroclastic despite Tora-Koshe –Dugdaridger is deep, no shallow ground water is available in this zone and this zone has deep confined fracture aquifer
- Lacustrine sediment mixed with pyroclastic fall deposited of Ziway is a major aquifer in the Ziway plain it is thick over 260m thickness and important unconfined aquifer in the study area.

2/Groundwater flow system and hydrochemistry of Ziway –Koka corridor in the main Ethiopian rift **(**Abiyu Kebede, 2008) presented in his MSC thesis.

- In this MSC thesis studies field well inventory, bore hale history and hydrochemistry of integrated methodology and approach were conducted to observe the ground water flow system and to determine hydrochemistry of the corridor .the thesis work report includes the following conclusion.
- Aquifer in the study area has two system the shallow and the deep. The shallow formed near to the surface up to 60m.depth and the deeper aquifer runs from nearly 63mto 268m as it was confined from lithological log and borehole data.
- Aquifer formation are classified in to four hydro stratigraphic units, lacustrine deposit, basaltic formation differentiated ignimbrite and welded tuffs units and rift volcanoes and volcanic ridges.
- In the deeper case ground flow clearly observed when it migrates from southern to northern part of the corridor.
- It was believed that this water movement is a part of ground water that migrates regionally from south part of the lakes region to the part of rift around afar.
- In the vicinity of Ziway lake the main recharge are is eastern part from which water migrated to lake Ziway with help of extensive structures that facilitate fast circulation and movement of ground water and other part of lake discharge water to the northern western and north western part from the shallow aquifer system.
- The two lakes (Ziway - Koka) have no interaction in the shallow (60m)and deep aquifer (>63M) system but considering the flow system obtained from hand dug well in the

vicinity of lakes the ground water flows from the lake to vicinity of very shallow depth hand dug well b/s of topographical variation.

- Fluoride vertical and lateral distribution has been studied in this thesis work in most part of the research area the fluoride concentration is high beyond the WHO standard(1.5gm/l)
- The concentration of fluoride in the shallow well (60m) higher than the deeper one (>63m), the fluoride concentration in the shallow well shows higher concentration (>19gm/l) but in the deeper case its concentration lowering down below 5mg/l.

3/ Geochemical and isotopic composition of natural water in the central main Ethiopia rift emphasis on the study of source and genesis of fluoride (Tewodros, 2006-2008)

- The chemical and mineralogy composition rocks results of fluoride indicated that the prevalent volcanic rock and rhyolites (i.e. felsic magmas) and that the fluvial volcano lacustrine sediments, represents the weathered (re-deposited).
- The microprobe result also showed that most of fluoride budget is concentrated in the glassy matrix. Glassy matrix is easily affected by weathering process that induces the neo formation of clay minerals that can potentially trap fluorine.
- This implies that the weathering products of these volcanic rock i.e. clay rich fluvial-volcano, lacustrine sediments are enriched in $F^-$with respect to the original mother rock.
- To verify the mentioned process the researcher performed laboratory leaching –tests on representative litho types out cropping in the rift valley. the powdered sampled were mixed with distilled water having a PH of about 5.5mg/l at ratio of 1.5(10g/50ml); room temperate) and shake for 12 months at frequently of 100rev/min the experiment was carried out in closed system i.e. utilizing closed plastic bottles which do not allow interaction with atmosphere gases. The concentration of fluoride of F^-in real natural water can be higher than those recorded in the experimental leachates.
- The concentration of F^-in experiment leaches is expected to increase with increase of time.
- the higher temperature and introduction of carbon dioxide have to be considered as additional factor favoring high fluoride in the natural water of the rift .these tests that simulate the water rock /sediment interaction processes experiment also conducted on volcanic ash (vitric ash) material after separating in to different grains size fraction (fine

ash, coarse ash and raw ash) to characterize the behavior of fluoride under flushing of synth entrain water. The result showed that high concentration of fluoride were leached out particularly from the fine ash fraction which turns suggest pyroclastic material are ultimate reservoir of fluoride

4/ Evaluation of water source of Meskan Marko and Silte Plain ground water basin for irrigation (WWDSE, 2015)

- On this project work investigation of ground water potential of the area will expand its view and make exploration and evaluation of ground water resource from volcanic rock aquifer such as basalt rhyolite trachyte and ignimbrite. The evaluation of ground water resource will be undertaken by on reliable methodology for data collection, review of privies work, carrying out field survey; identification, selection and evaluation of well field.
- The overall scope of the studies to determine the hydrogeological condition of the area: recharge and discharge conditions, delineate spatial distribution of different aquifers, hydraulic parameters and water quality of the aquifers and impacts of future exploitation of the potential aquifers.

1.6. Methodology and Instrumentation

Th**e** methodology used in this thesis work involves two phases:

The initial phase is basically assessment of previous studies and there validation of the main findings as a starting framework. background information on the geological , geophysical and hydrogeological aspect of the study area were obtained from a report entitl**e “**Evaluation of water resource of Meskan, Mareko and Silte plain groundwater basin for irrigation development project”(WWDSE, 2015) the report, composed of three phases, includes V-1 geological report, V-2, geophysical report, V-3 hydrological report.

The second phase involves data acquisition, processing and interpretation of the geophysical data in light of the existing background information harvested from the initial phase of (WWDSE, 2008).In the resistivity sounding survey using Schlumberger array total of 23 VES data along the traverses of Ziway- Butajra and Meki –Midre Kebd were collected in order to understand the general subsurface electrical stratification of the area, from which the different geological layers can be identified. This result is expected to give information on the shallow and deep ground water flow systems.

The unit utilized for the survey is the IRIS Syscal R1 plus Switch 72, Earth Resistivity Meter working in "Rho Mode". A four electrode array system was used in which two of the electrodes are used to introduce current in to the ground.

Thirteen (13) of these sounding measurements were on the Ziway Butajira traverse while the remaining ten (10) were on Meki- MedreKebd traverse. Sounding locations were taken with GPS.

For the sounding the position of the electrodes is moved out wards from the center of the profile to increase the depth of penetration of the sounding (the depth of penetration being equal to AB/2) the AB/2 distance was varied from 1.5 to 750m there were instance when the MN distance has to be increased to ensure the potential difference large enough to be measured with accuracy and so MN spacing were gradually increased from 0.5 to 45m overlap measurement were taken with every change in MN spacing.

VES measurements were subsequently plotted on a log lo g paper (apparent resistivity VESAB/2 in the field to determine bad data and there by facilitate repeat measurement in real time) in the field as the data were collected.

The other geophysical survey method employed in the work is the AMT survey. The magneto telluric (MT) method also has been introduced and applied in geophysical and structural geology prospecting it consists of the simultaneous measurement of orthogonal and magnetic natural field at any point on the surface of the earth in order to deduce the resistivity of rocks.

The AMT data were collected along four profiles following the same lines as the VES data, i.e. the Ziway - Butajira and Meki Miderkebde road traverse using the Geometrics STRATAGEM EH-4.

This unit capable of measuring electrical depth ranging from a few meter to more than 1km, with orthogonal electrical and magnetic field changes in the frequency range of 92 kHz and 10 KHz. These data were processed to provide tensor impedance measurement for interpreting complex 2D structure

This system is unique in that it uses both natural (in all measure frequency range) and controlled source electromagnetic signal however natural signal are generally weak in the higher fre9uency range this problem was solved by a transmitter located around some way from the receiver to strengthen the weak back ground field signal at higher frequency .the choice of the direction of profile and the implementation station has been made on the basis of the available geological information on the study area .the orientation of the major tectonic line as well as fault assumed to be observed in the study zone.

Table (1.1) GPS location sounding point the study are

GPS location of sounding points, UTM (m)							
Ziway-Btajira Traverse				**Meki-Midrekebd Traverse**			
VES NO.	**EAST**	**NORTH**	**ELEV. (m)**	**VES NO**	**EAST**	**NORTH**	**ELEV. (m)**
1	466159	877022	1662	1	477687	900432	1668
2	463495	877675	1666	2	474829	901242	1692
3	459684	881034	1849	3	471826	902104	1708
4	457903	884101	1769	4	468678	903006	1733
5	455513	884678	1807	5	464803	903551	1791
6	453703	885246	1814	6	461129	902874	1826
7	450004	885809	1873	7	459138	904758	1844
8	446457	887221	1824	8	458306	907110	1870
9	443154	889981	1835	9	459561	910631	1923
10	441082	894395	1842	10	458808	913499	1984
11	440286	896698	1864				
12	436990	898828	1956				
13	434392	897980	2025				

CHAPTER TWO

GEOLOGICAL AND HYDROGEOLOGICAL REVIEW

2.1. Regional Geological Setting

The major geological formation and tectonic features of the research of the research area were adapted from (Federal Democratic republic of Ethiopia water work and design and supervision Addis Ababa, 2015)

Lithospheric extension in Ethiopia is accompanied by intense volcanism ranging in age from Eocene to late Oligocene. The Oligocene to present volcanism of Ethiopia covers an area greater than 600,000 km^2. It is dominated by basaltic lavas and by rhyolite candy trachytic pyroclastic products and minor lavas. The Earliest recorded volcanic activity took place 40-45Ma in southern Ethiopia. Flood basalts forming the Ethiopian plateau were erupted between 33 and 28 MA. The second episodes of flood basalt volcanism were erupted between 18 and 11 Ma in southern Ethiopia rift and in the Main Ethiopian Rift and Afar at CA 10 Ma. After these episodes of pre-rift volcanic activity, with widespread flood basalts and subordinate felsic products, the onset of major rifting in different sectors of MER associated with bimodal Quaternary volcanism, with predominant felsic products and associated basalts takes place (Abebe et al., 1988, and references there in).

The volcanic rocks rest upon Mesozoic marine sedimentary sequences or directly on the Precambrian metamorphic basement. Studies on Ethiopian volcanism distinguish ad three main stages of volcanic activity. The first one is Oligocene to Miocene in age and was characterized by eruption of large flood lava sequences (known as Ashange and Aiba Basaltic Formations) forming the Ethiopian basaltic plateau. Latest phases of this stage were characterized by alternating basalt and ignimbrite eruption, forming the so-called Alaji Rhyolite Formation.

A second stage of activity is Miocene in age and is characterized by the construction of huge basaltic shield volcanoes (Tarmaber Basalt Formation).

The third stage is Pliocene to Quaternary in age and is directly related to the main phases of opening of the MER and Afar. In the Ethiopian rift, volcanism is dominated by per alkaline rhyolite ignimbrites and pumice and ash-fall deposits, with minor lava flows. Silicic rocks are associated with volumetrically subordinate basaltic products that form cinder cones and lava flows mostly aligned along extensional faults of the WFB (B. Abebe et al., 2007and references therein).The general Quaternary volcano-tectonic setting of the MER is controlled by the en-echelon arrangement of the Wonji Fault Belt (WFB; Mohr, 1962).

2.2 Local Geology

2.2.1 Lithology and Stratigraphy

2.2.1.1 Pre rift unit

The project area is covered with volcanic rocks and lacustrine sediments flooring the rift (Figure 2). . Crystalline basement and Mesozoic rocks are exposed only at the foot of Guraghe Mountain (western escarpment) near Kella town. The mapped units starting from the oldest to the youngest described in three phases; pre-rift, sync-rift, and main rift rock unit.

Pre-Tertiary rocks

a. Precambrian Basement rock

Pre tertiary units include Precambrian Basement rock and Mesozoic rocks. The Precambrian basement is highly weathered, yellowish brown, coarse grained gneiss. Microscopically, it is composed of orthoclase, biotitic quartz with inter-granular texture. This unit has an exposed thickness of more than 100m near to Kella.

The Mesozoic rock has about 30 m thick limestone overlying about 200 m thick sandstone near Kella town. The stratigraphic sequence includes:

- Compact greenish grey Ignimbrite
- Triassic Adigrat sandstone, reddish brown medium grained, 200m
- Shales and marls, ~30m thick

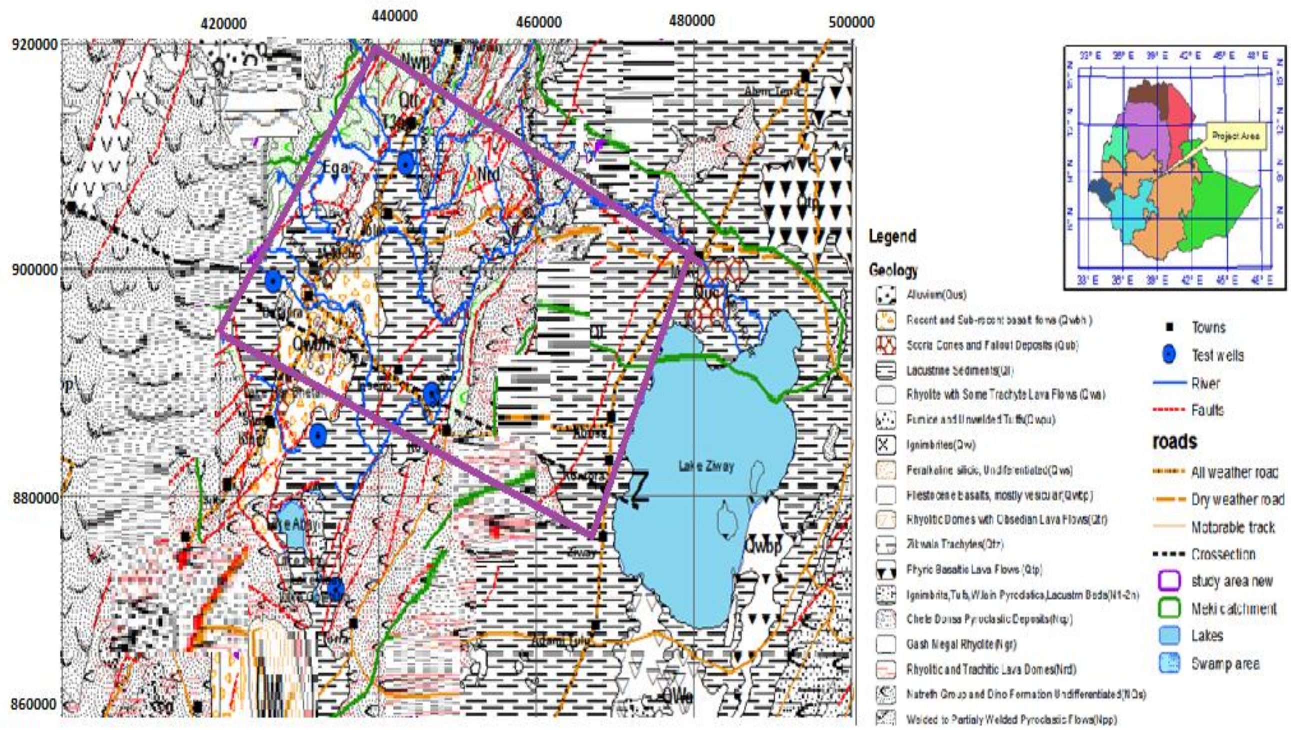

Figure 2.1 Geological map the study area (adopted from WWEDS, 2015).

b. Tertiary Rocks

The tertiary rock units include Aiba and Alaje Basalt, Anchar basalt and TarmabaMegezez basalt. Aiba and Alaje Basalt have basically identical mineralogy. Alajae rhyolite (also includes basalt that is inter bedded frequently) overlies Aiba basalt which is underlain by Ashangi basalts, a sequence which is faulted, fractured and tilted.

Anchor basalt mainly basaltic and to a minor extent rhyolite-sequence overlies the Lower Plateau and underlies the Pliocene silicic sequences. It outcrops only in the western margin in correspondence with the Guraghe escarpments (Abebe et. al, 2005). This sequence consists of pyric to plagioclase and pyroxene pyric basalts and trachyte basalt intercalated with rhyolite tuffs. It is estimated to be more than 300 m thick in the Guraghe Mountains.

In fresh samples, it is dark grey, hard and compact in appearance, but reddish brown in weathered ones. It is medium to coarse grained rock composed of plagioclase, pyroxene, and opaque minerals.

The other basalt of the tertiary volcano, Tarmaber basalt is dominated by transitional to Na-alkaline basalts with minor benmoreites and trachyte's (Piccerillo et al., 1979). It is fine grained and dark gray color. Petrographic ally it is composed of plagioclase, pyroxene and opaque minerals. Tarmaber basalts in contrast to tholeitic and mildly alkaline nature of the earlier flood basalts are typically alkaline in nature.

2.2.1.2 Rift Units

Rift Shoulder

This unit is the dominant unit in the mapped area. It covers a wide area and it represents the most extensive regional salicylic unit in the area. It exposed along the Guraghe escarpment. The maximum estimated thickness of this unit is ~700m along the rift escarpments at Guraghe.

a) Welded Pyroclastic Flows

This unit in the mapped area exposed at the foot of mount Guraghe and it extends towards the northern and eastern part of the mapped area. It is light to dark-grey in fresh samples and reddish to yellow to pink in weathered ones. It is coarse grained, densely welded rock containing vitrophyric fiamme and

Lithic fragments with associated rhyolite lava flows interleaved with ash and unwedded tuffs. Microscopically, it consists of crystals of K-feldspar (sanding), quartz, plagioclase and hornblende having vitrphyric texture.

b) **Welded Pyroclastic Deposit Inter-bedded With Basaltic Lava Flows**

This unit mainly crops out in the western margin of the MER (along the Guraghe escarpment). The formation forms ridge and has light to dark brown in color, coarse grained, welded rock unit associated with dark, fine grained basaltic lava flows.

c) **Welded to Partially Welded Pyroclastic flows**

This rock unit covers a wide area on the top of Guraghe Mountain. The unit also exposed northern part the mapped area .It has light gray color, fine to medium grained welded to partly welded pyroclastic deposit associated with rhyolite lava flows interlayer with ash and tuffs. Petrographic study shows, the unit is composed of K-feldspar, quartz and plagioclase minerals.

2.2.1.3 Inner Rift

a) Rhyolite Lava Domes and Flows

This unit is exposed in northern and eastern part of the mapped area. It is light gray to pink in color composed of alkali feldspar, quartz and mica. This unit forms caldera and small domes and broad-based gentle sloping circular to elliptical hills. Locally, it shows intercalation of fine ash and unwedded tuffs. Microscopically, it consists of feldspar (sanding), quartz, muscovite with rhyolite texture.

a) Pumice and Un-welded Tuff Deposits

Exposure of this unit is found in south eastern portion of the mapped area. It is light grey, fine-grained, poorly welded rock containing vitrophyric fiamme and lithic fragments with associated rhyolite lava flows interleaved with pumice, and unwedded tuffs. Microscopically, it consists of crystals K-feldspar (sanding), quartz, plagioclase and hornblende having vitrphyric texture.

b) Ignimbrite

This unit crops out in central east, northern and southern part of the mapped area. It is widely exposed in Medrekebd Abo Monastery area. It is also exposed in Koshe area forming ridge. It has light to dark-grey color in fresh samples and greenish dark in weathered samples. It is coarse grained, poorly welded rock containing vitrophyric fiamme and lithic fragments with associated rhyolite lava flows interleaved with ash and unwedded tuffs. Microscopically, it consists of crystals of K-feldspar (sanding), quartz, plagioclase and hornblende having vitrphyric texture.

c) Quaternary Basalt &Scoria Fall Deposit

This unit ropes out in the western part of the mapped area around Butajira area. It is restricted to a narrow marginal graven (Gidey WoldeGabrielet al., 1990) and is marked by NNE–NE-aligned cinder cones, maars and some lava aprons. The basalt unit is dark color, fine-grained, vesicular and it is associated with red scoria rock mainly composed of plagioclase, pyroxene and opaque minerals and their texture varies from pyric to porphyritic. . Generally, it is fresh, compact fine grained rock, but in places, it shows vesicular cavity filled with or without secondary minerals.

d) Lacustrine Sediment

This unit is exposed in eastern and central part of the mapped area occupying the rift floor at elevation below 1900m above sea level. It is composed of loose, light to yellowish grey color sand and silt size sediments. The major components of these sediments are of volcanic origins, such as pumice, volcanic ash, obsidian, rhyolite and basalt rock fragments.

e) Chefe Donsa Pyroclastic Deposits

This unit includes pyroclastic deposits overlying the Nazret Pyroclastic Rocks and. in some localities. Bofa Basalts. The Chefe Donsa Pyroclastic deposits consist of unwedded to poorly weld. Fine volcanic ash flow and fall deposit composed of mainly comenditic rhyolites. The poorly welded sequence of the Chafe Donnas Pyroclastic is easily differentiated from the generally strongly welded Nazret Pyroclastic. The Chefe Donsa Pyroclastic Deposits are almost completely contained in the rift floor. They are well exposed along the borders of the rift margin above 1900 m. whereas below this elevation they are generally covered by the lacustrine sediment and are exposed only in some river gorges. Some big caldera forming central volcanoes such as Boku, Haya, and Gademotta (the latter located south of the map area) have age ranges that generally overlap with those of the Chefe Donsa Pyroclastic Deposits. Thus, although an origin of local fissures for these deposits cannot be excluded, these large caldera structures may represent the main sources for these pyroclastic products. The exposed thickness of these pyroclastic varies from 0 to 40 meters.

In General the whole section starting from the Gurage mountain is occupied mostly by Nazret group volcanic comprised by welded to partially welded pyroclastic, welded pyroclastic lacustrine deposit, Chefedonsa pyroclastic, Rhyolite tuff with welded tuff and recent to sub recent basalt.

f) **Rhyolite tuff and welded tuff**

This unit is not recorded on surface and is not depicted on the geological map altogether. However, separate units of rhyolite flow and welded to partially welded rock is found on the map. In this case the two rocks were encountered interchangeably below 247 m at Koshe.

2.3 Geological Structures of the Study Area

The geological structures observed in the project area are joints, fractures, lineaments and faults. These structures are associated with tectonic and magmatic features of the Ethiopian Main Rift and the youngest Wonji Fault Belt system of faults.

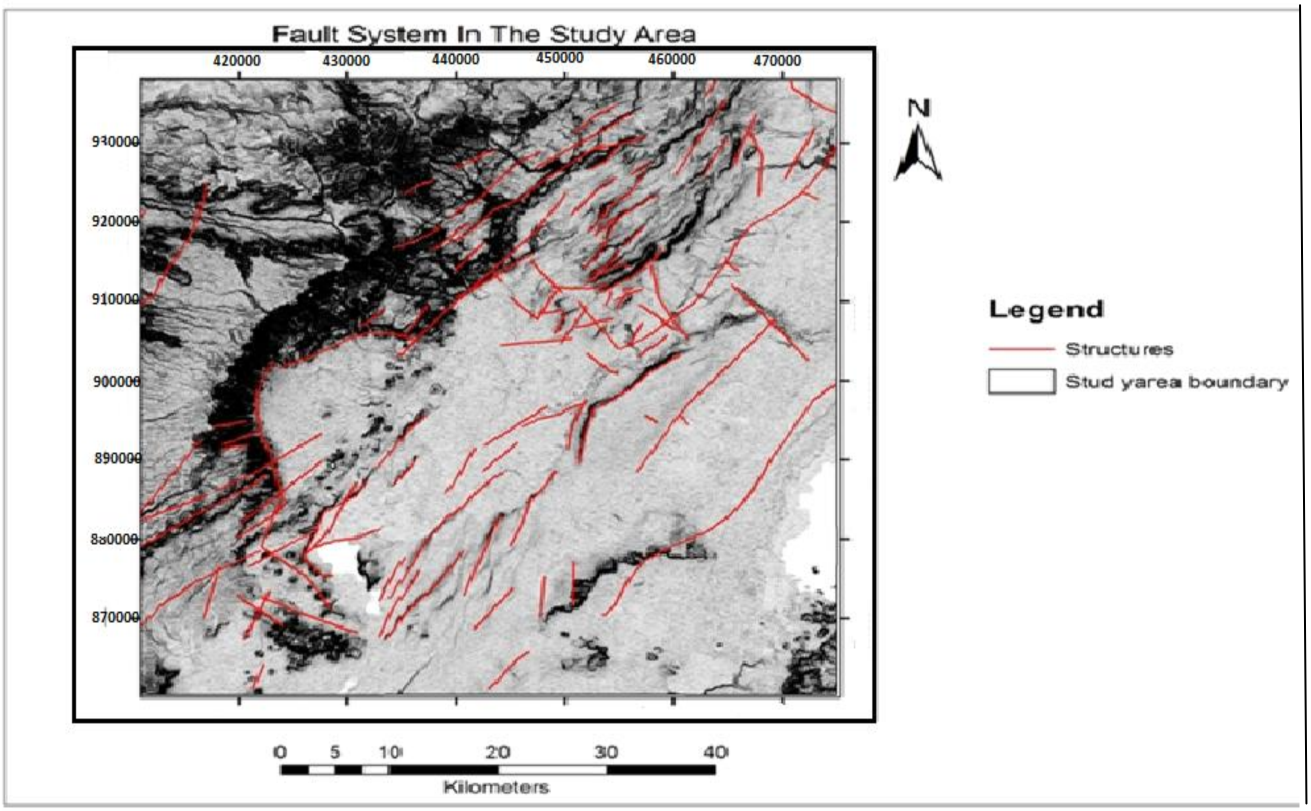

Fig 2.2Geological structure of the study area (adapted from WWDSE 2005)

2.3.1 Fault System

The study area structural pattern is characterized by two main fault systems a roughly 030^{o}-040^{o} trending border fault system and a 000^{o}-020^{o} trending fault system (WFB) mainly affecting the rift floor (Mohr, 1962, 1967, 1987; Gibson,1969; Mohr and Wood,1976; Kazmin et al., 1969; Boccaliti et al., 1992, 1998; Chorowiczet al., 1994).Despite the overall NE-SW trend of the MER, the WFB is characterized by active NNE-SSW trending extensions fractures and normal faults .The western section of the mapped area is characterized by 025^{o}-045^{o} trending border fault system separating the Ethiopian plateau from the rift floor. These faults are characterized by major rift escarpments, exceeding 1000m in heights around Guraghe Mountain (west of Butajira). Syn-rift volcanic units crop out in N-S trending MedreKebd structural high at western margin are affected by NE- SW trending faults .This structural high give rise the Butajira embayment.

The rift floor is strongly affected by dense fault swarms individual fault exhibits relatively small throws and strike ~20^{o} counterclockwise from the regional trend of the rift margin. These faults have steep scarps and have right stepping arrangement of an echelon 000^{o}-020^{o} trending faults of the WFB. These structures give rise to a wide spread deformation the rift floor. These NNE–NE Quaternary rift zones of the WFB form areas of activate formation obliquely cutting the rift floor in the MER. Even though without exposed faults, the Butajira volcanic field constitute further off-axis belts of Quaternary activity, located on the western margin of MER. The Butajira volcanic zone is restricted to a narrow marginal graven (Gidey WoldeGabriel et al., 1990) and is marked by NNE–NE-aligned cinder cones, maars and some lava aprons devoid of exposed fault.

2.3.2 Lineaments

These are either linear or curvilinear features observed in the map area. They are traced following ridge crests and river channels and are from few centimeters to tens of centimeters long in the map. They have variable trend; NW-SE, NE-SW, N-S and E-W. The NE-SW trending lineaments appear to be more dominant than the others.

2.3.3. Foliation

The mapped area is featured by preferred alignment of flaky (biotitic, muscovite) minerals and amphibole (hornblende) crystals and stretching of quartz and feldspars parallel to the general strike of the rock body. This is well seen in gneiss having a NW-SE direction dipping 32° north east (Di Paola and TesfaMichael Berhe, 1978).

2.3.4 Joints and fractures

Joints: they are produced as a result of contraction that accompanies cooling of hot volcanic deposits and high level intrusions. Types of discontinuity plane in the mapped area are columnar joints, concentric joints, and tiny normal joints of which columnar and tiny commonly observed.

CHAPTER THREE

GEOPHYSICAL METHODS

3.1 General Considerations

Geophysics studies properties of the earth and its internal constitution from the physical phenomena associated with it by applying the principle of physics. Measurements of electrical resistivity are made with circuit in which the earth is one of the components, namely resistor. The procedure is attained by passing a measured amount of electric current through a segment of the earth and then measure the potential difference associated with the current. Using the measurement of contrasts in the physical properties of materials beneath the surface of the earth and attempt to deduce the nature and distribution of the materials or bodies with in the earth that are amenable to measurement like resistivity, density, magnetism, rigidity, compressibility, etc. The measurements can be made in a variety of ways to determine a variety of results. In the field lay out the electrodes are either expanded outward about a center point which is Vertical Electrical Sounding (VES) or on the other hand, the field lay out moves along a profile keeping a fixed distance between the electrodes, to study the lateral changes in electrical resistivity known as profiling.

Geophysical interpretations are mostly remote inference about the observed physical property. However, when appropriate subsurface investigations are integrated with geophysical measurements, large volumes of material can be explored both accurately and cost-effectively

3.1.1 Theoretical Basis

3.1.1.1 Geoelectrical Methods

The theory and field methods used for resistivity surveys are based on the use of direct current, because it allows greater depth of investigation than alternating current and because it avoids the complexities caused by effects of ground inductance and capacitance and resulting frequency dependence of resistivity An electrical method of investigation in relation to structural mapping used to determine the litho logical succession and the possible water bearing horizons in terms of resistivity and depth.

3.1.1.2 Potential Distribution in the Earth

For a particular arrangement and spacing of electrodes an equation giving the apparent resistivity in terms of applied current, distribution of potential, and arrangement of electrodes can be arrived at through an examination of the potential distribution due to a single current electrode. The effect of an electrode pair or any other combination can be found by superposition (Flathe, 1964). Consider a single point electrode located on the boundary of a semi-infinite, electrically homogeneous medium, which represents a fictitious homogeneous earth. Because air has infinite resistivity, no current flows upward so as to define hemispherical surface. If the electrode carries a current, I, measured in Amperes, the potential at any point in the medium or, on the boundary is given by;

$$V = \rho \frac{I}{2\pi a} \tag{3.1}$$

Where V is the potential in Volts, ρ is the resistivity of the medium and "**a**" is the distance from the electrode.

Equation 3.1 is the fundamental equation in Electrical resistivity prospecting and it is possible to use it to develop more practical relationships. The potential at a point of infinitely far away by convention is arbitrarily defined to be equal to zero. Thus, at distance 'r' from the current electrode 'a', the regions possess the same potential whose surfaces are known as equipotential surfaces (Figure 3.1). They represent imagery shells, or bowls, surrounding the current electrodes, and on any one of which the electrical potential is everywhere equal.

To find a practical method of determining the resistivity's of the layers and the depths of the boundary planes mathematical relation between the measured quantities and the parameters that define the layer distribution in the surface (Otto, 1879).

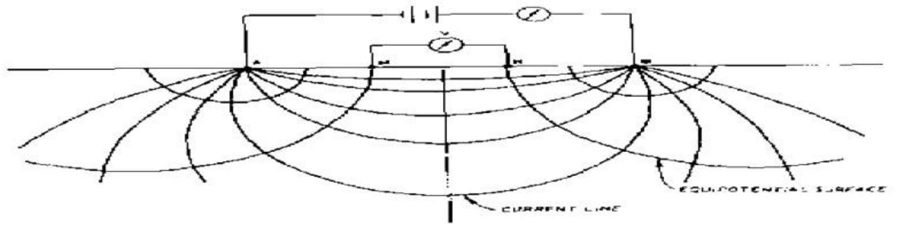

Figure 3.1 Electric field distribution around a current source over homogeneous media.

This problem can be simplified by the following assumption:

- The potential field about the vertical axis of the current source is axially symmetric and the potential is additive.
- The subsurface consists of a finite number of layers separated by horizontal boundary planes.
- The field is generated by a point source of current located at the surface.
- The deepest layer extending to infinite and each of the layers is electrically homogeneous and isotropic.

The electrical potential V for DC (direct current) satisfies the differential equation of Laplace (Otto, 1879).

$$\nabla^2 V = 0 \tag{3.2}$$

$$\frac{\partial^2 V}{\partial x^2} + \frac{\partial^2 V}{\partial y^2} + \frac{\partial^2 V}{\partial z^2} = 0 \tag{3.3}$$

Since the potential field has a cylindrical symmetry about the vertical axis passing through the point delivering the current, one should preferably use Laplace equation in cylindrical coordinate, i.e.

$$\frac{\partial^2 V}{\partial r^2} + \frac{1}{r}\frac{\partial V}{\partial r} + \frac{\partial^2 V}{\partial z^2} + \frac{1}{r^2}\frac{\partial^2 V}{\partial \theta^2} = 0 \tag{3.4}$$

For a solution symmetrical with respect to the vertical axis, $\frac{dv}{d\theta} = 0$ *and* $\frac{d^2v}{d\theta^2} = 0$ *so* equation

$$\frac{\partial^2 \mathrm{V}}{\partial r^2} + \frac{1}{\mathrm{r}}\frac{\partial \mathrm{V}}{\partial \mathrm{r}} + \frac{\partial^2 V}{\partial z^2} = 0 \tag{3.5}$$

The particular solution of equation 3.5 is obtained from method of separation of variables by making the assumption that there exist solutions that have the form;

$$V(r, \mathrm{z}) = U\,(r)\;W\,(\mathrm{z}) \tag{3.6}$$

Substituting equation (3.6) into equation (3.5) yields;

$$\mathrm{W}(\mathrm{z})\frac{d^2\mathrm{U}(\mathrm{r})}{dr^2} + \frac{1}{\mathrm{r}}W(\mathrm{z})\frac{\mathrm{dU}(\mathrm{r})}{\mathrm{dr}} \tag{3.7}$$

$$+\mathrm{U}(\mathrm{r})\frac{d^2\mathrm{W}(\mathrm{z})}{dz^2} = 0$$

Dividing throughout by U(r) W (z) gives;

$$\frac{1}{\mathrm{U}(\mathrm{r})}\frac{d^2\mathrm{U}(\mathrm{r})}{dr^2} + \frac{1}{\mathrm{U}(\mathrm{r})\mathrm{r}}\frac{\mathrm{dU}(\mathrm{r})}{\mathrm{dr}} \tag{3.8}$$

$$+\frac{1}{\mathrm{W}(\mathrm{z})}\frac{d^2\mathrm{W}(\mathrm{z})}{dz^2} = 0$$

Equation (3.8) is satisfied if and only if

$$\frac{1}{U(r)}\frac{d^2U(r)}{dr^2}+\frac{1}{U(r)r}\frac{dU(r)}{dr}=-\lambda^2 \tag{3.9}$$

And

$$\frac{1}{W(r)}\frac{d^2W(z)}{dr^2}=\lambda^2 \tag{3.10}$$

Where λ is an arbitrary real constant?

The solution of equation (3.10) can be written as

$$W(z)=C_2e^{-\lambda z} \quad \text{and} \quad W(z)=C_3e^{+\lambda z} \tag{3.11}$$

The solution of equation 3.9 is;

$$U(r)=CJ_0(\lambda r) \tag{3.12}$$

where J_0 is Bessel function of order zero.

Combining equation (3.11) and (3.12) gives the particular solutions of a differential equation (3.5);

$$V(r,z)=Ce^{-\lambda z}J_0(\lambda r)\text{and } V(r,z)=Ce^{+\lambda z}J_0(\lambda r) \tag{3.13}$$

where C and X are arbitrary constants.

However any combination is also a solution of differential e9uation thus by making λ to go through all possible value from 0---∞ and allowing the two Constance C to very independent of λ, the general equation (3.5)

$$V(r,z)=\int_0^\infty\left[\emptyset(\lambda)e^{-\lambda z}+\psi(\lambda)e^{+\lambda z}\right]J_0(\lambda r)d\lambda \tag{3.14}$$

In equation (3.14) both ϕ (λ) and ψ (λ) are arbitrary function ofλ.

From the basic theory of the potential generated by a point source of current of intensity I, located at a point p is given by

$$V(r,z) = \frac{\mathrm{I}\rho}{2\pi}\left[\frac{1}{\sqrt{r^2+z^2}}\right] \tag{3.15}$$

To write equation (3.15) can be written in Lipchitz integral formula that is;

$$\left[\frac{1}{\sqrt{r^2+z^2}}\right] = \int_0^\infty e^{-\lambda z} J_0(\lambda r)d\lambda \tag{3.16}$$

So that equation (3.15) can be written in the form of

$$V(r,z) = \frac{\mathrm{I}\rho}{2\pi}\int_0^\infty e^{-\lambda z} J_0(\lambda r)d\lambda \tag{3.17}$$

The general solution of differential equation (3.14) can now be written in the for

$$V(r,z) = \frac{\mathrm{I}\rho}{2\pi}\int_0^\infty \left[e^{-\lambda z} + \theta(\lambda)e^{-\lambda z} + X(\lambda)e^{+\lambda z}\right]J_0(\lambda r)d\lambda \tag{3.18}$$

whereθ_i (λ) *and*χ_i (θ) are arbitrary functions ofλ.

The solutions the forms of equation (3.18) are valid in all layers of the subsurface. The function θ_i (λ) *and*χ_i (θ) may not take the same form in each of the layers in the subsurface (Otto, 1879).

In the case of the a point source of current at the surface of a horizontally layered earth we must thus write separate expressions for the solution in different layers that is;

$$V_i(r,z) = \frac{I\rho_i}{2\pi}\int_0^\infty \left[e^{-\lambda zi} + \theta_i(\lambda)e^{-\lambda z} + \chi_i(\lambda)e^{+\lambda zi}\right]J_0(\lambda r)d\lambda \tag{3.19}$$

Equation (3.19) is called Stefansson integral and the subscript “i” refers to several layers of the Subsurface.

3.1.1.3 Electrical Properties of Rocks

Surface electrical resistivity survey is based on the distribution of electrical potential in the ground around a current-carrying electrode which depends on the electrical resistivity and distribution of the surrounding rocks and soils. This is because of the fact that all materials, including soil and rock, have an intrinsic property, called resistivity that governs the relation between the current density and the gradient of the electrical potential. The propagation of electric current in rocks and minerals may occur in three ways. These are Electronic (Ohm), Electrolytic and dielectric conduction (William, 1997).

The first is the normal type of current flow in materials containing free electrons, such as the metals. In an electrolyte the current is carried by ions at a comparatively slow rate. Dielectric conduction takes place in poor conductors or insulators, which have very few free carriers or not at all.

Variations in the resistivity of earth materials, also called an anomalous resistivity, which may be due to discontinuity of rock formation or change in physical condition perturbs the distribution of current or potential lines compared to their pattern of a homogeneous earth and thereby reveal something about the composition

Extent and physical properties of rocks and soils in the subsurface (Flathe, 1964). Since in most rock materials the porosity and the chemical content of the water filling the pore space are more important in governing resistivity than grains of mineral which the rock itself is composed.

The resistivity of rocks is also strongly influenced by the presence of ground water, which acts as an electrolyte. Due to the good electrical conductivity of ground water the resistivity of sedimentary rock is much lower when it is water logged than in the dry state. Very roughly, igneous rocks have the highest resistivity, sediments the lowest, with metamorphic rocks intermediate; however, there is a considerable overlapping of different rocks (Telford et al., 1976).

3.1.1.4 Apparent Resistivity

Apparent resistivity is defined as the resistivity of an electrically homogeneous and isotropic half-space that would yield the measured relationship between the applied current and the potential difference for a particular arrangement and spacing of electrodes. The apparent resistivity is definitely not an average value and only in the case of homogeneous ground it is equal to the actual resistivity (Telford et al., 1976). That means the

Resistivity determined would have been true resistivity if the ground were homogenous and isotropic. However, usually, the ground constitutes various materials and there may be some variations in the lateral or vertical dimensions and that is why we call an apparent resistivity. Its magnitude depends not only on the nature of the geologic system but also on the geometric dispositions of the electrodes used for the measurement (William, 1997).

3.1.1.5 Depth of Investigation

Depth of investigation is a depth that contributes most to the total signal measured on the ground surface it does not mean that the entire measured signal originated at that depth alone. The contributions for the measured signal may come from all depths, but the contributions from the depth of investigation are the largest. In that case, our depth of investigation is synonymous with the depth of the maximum contributions to signal (Telford et al., 1976). Therefore the depth of investigation is an important physical concept in any method of geophysical prospecting.

There is no simple relationship between the electrodes spacing at which curve has been reached features of the apparent resistivity curve are located and the depths to the interfaces between layers. The depth of investigation will always be less than the electrode spacing. Typically, maximum electrode spacing of three or more times the depth of interest is necessary to assure that sufficient data have been obtained. This governs the effective depth of investigation (Flathe, 1964).

3.2 The Principles of Equivalence and Suppression

3.2.1 The Principles of Equivalence

Equivalence refers to the condition in which different combinations of layer resistivity and thickness may lead to an apparent resistivity curves which are within the accuracy of observations indistinguishable although not identical. The Equivalence Problem may occur due to too low or too high values of the transverse resistance (T) or longitudinal conductance (S) caused by difference in the content of aquifer (Orellana and Mooney, 1966).Equivalence is controlled by the nature of the current flow for example for the VES method:

- Current flow perpendicular to thin resistive layer.
- Current flow parallel to thin conductive layer.

There is interplay between thickness and resistivity; there may be anisotropy of resistivity in some strata; large differences in geoelectrical section, particularly at depth, produce small differences in apparent resistivity; and accuracy of field measurements is limited by the natural variability of surface soil and rock and by instrument capabilities. As a result, different sections may be electrically equivalent within the practical accuracy limits of the field.

3.2.2 Suppression

Suppressions happen when the effect from the thickness of an intermediate layer is very small as compared to its depth. The test of geological reasonableness should be applied in particular; interpreted thin beds with unreasonably high resistivity contrasts are likely to be artifacts of interpretation than the real features (Telford, et *al.*, 1976).Adjustments to the interpreted values may be made on the basis of the computed VES curves and checked by computing the new curves. Because of the accuracy limitations caused by instrumental and geological factors, effort should not be wasted on excessive refinement of the interpreted.

3.2 The Magneto telluric Method

3.2.1 The Source of Magneto telluric Signals

The magneto telluric method uses natural electromagnetic signals to remotely sense the electrical resistivity structure of the subsurface. Since the depth of exploration is inversely related to the square root of the frequency, the MT method can be categorized into three distinct exploration regimes.

1. Long period MT data are used to image depths from 1-1000 km and use signals with frequency below 0.1 Hz. Resolution in the upper 1-2 km is low owing to the long wavelength of these low frequency signals.

2. Broadband MT (0.001 - 500Hz) is used for crustal scale studies.

3. Audiomagnetotellurics (AMT) uses high frequencies (10000 - 1 Hz) to study shallow structure. This gives resolution on scales of 10 - 1000 m and is thus most suited to mineral exploration.

At frequencies below 1 Hz, the EM signals used in MT originate in the ionosphere. These variations are caused by fluctuations in the strength and density of the solar wind. At frequencies above 1 Hz, the source is global thunderstorm activity, which propagates worldwide in a waveguide bounded by the conducting earth and ionosphere (Vozoff, 1991). As lightning strikes occur rapidly, AMT signals are generally present over quite a wide frequency band. However, signals can be weak in the so-called AMT dead band around 2 kHz, especially in the daytime.

3.3.2 Electromagnetic Wave Propagation in a Conductor

EM signals, generated outside the Earth, travel in the air as a wave. The amplitude decreases through geometric spreading but without attenuation. When these signals enter the Earth the non-zero conductivity of the Earth causes strong attenuation and the EM signals travel by diffusion. Their behavior can be described by Maxwell's equations:

$$\nabla . \mathbf{E} = \frac{\rho}{\varepsilon_0}, \nabla . \mathbf{B} = 0, \quad \nabla \mathbf{x}\, \mathbf{B} = \mu \mathbf{J} + \mu\varepsilon \frac{\partial E}{\partial t}, \quad \nabla \mathbf{x}\, \mathbf{E} = -\frac{\partial B}{\partial t} \tag{3.20}$$

Field is generated by free electric charges. The second equation is based on the observation that magnetic field lines must form closed loops and hence magnetic monopoles do not exist. The third equation is an expression of Ampere's Law and quantifies how much magnetic field (B) is generated by a specified electric current density (J). It also includes the displacement current term that was introduced by Maxwell. The fourth equation is Faraday's Law and its physical meaning is that a changing magnetic flux generates an electric field. To solve these equations, three constitutive equations must also be defined, i.e.

$$\mathbf{J} = \sigma \mathbf{E}, \quad \mathbf{B} = \mu\, \mathbf{H}, \quad \mathbf{D} = \varepsilon\, \mathbf{E} + \mathbf{P} \tag{3.21}$$

Where **D** is the displacement or the electric flux density and **P** is the polarization general, $\boldsymbol{\sigma}, \boldsymbol{\mu}$ and $\boldsymbol{\varepsilon}$ are constant in time but vary with position in the Earth.

For Earth materials μ and ε vary little from their free space values and thus can be assumed to be constant. The free space values for μ and ε are $\mu_0 = 4\pi 10^{-7}$H/m and $\varepsilon_0 = 8.85\ 10^{-12}\mathrm{F/M}$

The third and fourth Maxwell's equations can be coupled to give the following equation for **E**,

$$\nabla \mathbf{x}(\nabla \mathbf{x} \mathbf{E}) = -\frac{\partial}{\partial t}\left(\mu\sigma E + \mu\varepsilon \frac{\partial E}{\partial t}\right) \tag{3.22}$$

Is assumed that there are no free charges in the subsurface $(\nabla . \mathrm{E} = 0)$, then this

Expression can be simplified to

$$\nabla^2 \mathrm{E} = \mu\sigma \frac{\partial E}{\partial t} + \mu\varepsilon \frac{\partial^2 E}{\partial t^2} \tag{3.23}$$

The first term represents signals that travel by diffusion (conduction current) and the second term represents wave propagation (displacement current). Note, this equation assumes that the charge density (ρ) is zero. To solve equation 3.23 for the context of magneto telluric, some simplifications must be made. Firstly, it is assumed that the EM fields exhibit a simple harmonic time variation of the form $\mathrm{E} = \mathrm{E}_0 e^{-i\omega}$ where ω is angular frequency. The electric field, **E,** can be written as the product of two functions

$$E(x, y, z, t) = E_0(x, y, z) e e^{-i\omega t} \tag{3.24}$$

Do not vary with time. Substitution into equation (3.24) gives

$$\nabla^2 \mathrm{E}_0 + \omega\mu(i\sigma + \omega\varepsilon) E_0 = 0 \tag{3.25}$$

At the low frequencies used in MT, the current flow via conduction is dominant and the displacement ignored. Thus, it is assumed that all EM energy in the Earth travels by diffusion and the spatial variation of the electric field can be written as $E_0\ (x, y, z)$where:

$$\nabla^2 \mathrm{E}_0 + i\omega\mu\sigma E_0 = 0 \tag{3.26}$$

If it$\frac{\partial^2 E_x^0}{\partial z^2} + i\omega\mu\sigma\, E_x^0 = 0$ is no assumed that the incident wave is planar, polarized in the x-direction and propagating downwards in the z-direction, equation (3.26) can be simplified giving.

$$\frac{\partial^2 E_x^0}{\partial z^2} + i\omega\mu\sigma E_x^0 = 0 \tag{3.27}$$

To solve this equation a trial solution can be used of the form

$$E_x^0(Z) = Ae^{\lambda z} \tag{3.28}$$

Boundary conditions are applied such that $E_x^0 = E_s$ at $z = o$ and E_x^0 is bounded as z approaches can show that the solution has the form:

$$E_x^0(z) = E_x^0(z)e^{-zi\delta}e^{iz/\delta} \tag{3.29}$$

Where δ is called the skin depth (in meters) and is defined as

$$\delta = \sqrt{\frac{2}{\omega\mu\sigma}} = \sqrt{\frac{T\rho}{\pi\mu}} = 503.29\sqrt{\frac{\rho}{f}} \tag{3.30}$$

3.3.3 Interaction of EM Signals with a Uniform Earth

It can be shown that when an incident EM signal strikes the Earth's surface, most of the energy is reflected back into the air (Simpson and Bahr, 2005). Only a small fraction travels into the Earth. It can also be shown of horizontal electric and magnetic fields contains information about the electrical resistivity of the subsurface. This ratio is termed the impedance and it is a function of frequency

$$Z_{xy}(\omega) = \frac{E_x(\omega)}{H_y(\omega)} \tag{3.31}$$

For a half space, it can be shown that,

$$Z_{xy}(\omega) = \frac{-i\omega\mu}{k_1} \tag{3.32}$$

It follows that

$$Z_{xy}(\omega) = (1-i)\sqrt{\left(\frac{\mu\omega}{2\sigma}\right)} \tag{3.33}$$

The apparent resistivity can then be expressed as:

$$\rho_a(\omega) = \frac{1}{\omega\mu}\left|\frac{E_{x(\omega)}}{H_{y\,(\omega)}}\right|^2 \qquad (3.34)$$

Apparent resistivity in Equation (3.34) represents an average resistivity of the Earth from the surface to a depth equal to a skin depth. Another important parameter of the MT method is the phase which can be defined as the argument Φ of the impedance)

$$\arg\,(Z_{xy}) = \frac{\mathrm{IM}(Z_{xy})}{\mathrm{Re}\,(Z_{xy})} \qquad (3.35)$$

It is simple to show that:

$$\Phi \; = \tan^{-1}(-1) = \frac{\pi}{4} => 45^0 \qquad (3.36)$$

When an electromagnetic wave propagates in the air, there is no phase difference between the electric and the magnetic fields of the Earth. However, it is 45^{o} in a homogeneous, conduve.

Therefore, if the Earth has a uniform resistivity, the apparent resistivity and phase would be constant at all frequencies. In contrast, if the Earth has a more complex geo electrical structure then both the apparent resistivity and the phase will vary with frequency. A Comparison of homogeneous and two layer earth model AMT responses is presented in Figure 3.5

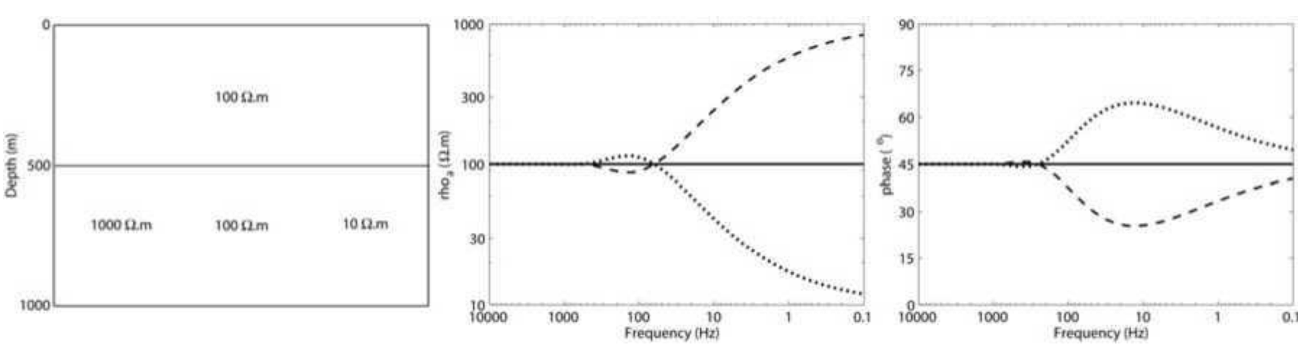

Figure 3-2. The subsurface electrical model (left panel) and associated resistivity (middle panel) and phase (right panel) curve.

CHAPTER FOUR

DATA ACQUISITION AND PROCESSING

4.1 Data Set and Survey Layout

Figure 4.1 shows the position of the VES and 2D MT data points used for this work. The 23 VES sounding are indicated by inverted triangle and the 26 2D MT points are indicated by circular dots. Moreover, four profile lines for the sounding data point and also four profile lines for the 2D MT measurement were chosen for this thesis work.

4.2 Processing and Interpretation of resistivity data

Data processing, the steps of preparing the field data for geophysical interpretation, often includes judgments and observations based on the experience of the processor. Interpretation of the data, as well as the planning of the survey, must be guided by the available knowledge of the local geology. The interpreter normally knows what he is looking for in terms of geological features. Interpretation is a continuous process throughout geophysical investigations and its adequacy is crucial to achieve the objectives (Zohdy, 1989).

The first step of the data processing is the transformation of the instrument responses, the source current strength and the potential difference, to apparent resistivity values using the relation;

$$\rho = \frac{K\Delta V}{I} \tag{4.1}$$

WhereΔV = potential, in Volt, K = geometric factor and ρ = resistivity of the medium, and

The main objective of quantitative interpretation of resistivity sounding data is to determine the thickness and resistivity of different horizon, from the measured field curves and use these parameters to obtain the geo-electric stratification of the area under investigation. Quantitative

Figure 4.1 Location map of the sounding (VES and MT) points overlaid on the digital elevation model (DEM) of the study area.

Interpretation in resistivity work usually involves the use of direct and inverse modeling. From a given set of layer parameters, it is always possible to compute the apparent resistivity as a function of the separation of current electrodes.

Preparation of geophysical models always assumes the following:

(I) Earth materials have distinct subsurface boundaries.

(II) A material is homogeneous (having the same properties throughout).

(III) The unit is isotropic (properties are independent of direction).

In this research work three interpretation procedures were applied, namely: two layer curves matching with master curves and auxiliary point charts. Direct correlation with available borehole data and computer matching technique by an iterative least squares inversion program Win-resist (Win-resist Version 5.1, 1981-2001).

Before the availability of personal computers, the curve matching process was done graphically by plotting the field data plotted on transparent log-log graph paper at the same scale of catalogs of two-and three-layer standard curves. The use of standard curves requires an identification of the curve type followed by a comparison with standard curves of that type to obtain the best match, Auxiliary Point Method, which requires the use of small set of auxiliary curves and some constructions. This method is very important, in that it can be used to interpret, in principle, any number of layers by alternate use of two layer master curves, which is done by matching the initial branch of the field curve with an appropriate two layer master curve and a family of auxiliary point curves that correspond to the field curve type. Therefore, rough estimation based on segment by segment matching will be the best that can be done. The process is controlled by using those auxiliary curves to define allowable positions of the origin of the two-layer curve being fitted to the latter segments of the field curve. The first approximations of the layer parameters were thus obtained through the above method (Zohdy, 1989).

The inversion of VES data is nonlinear inversion and hence the determination of the model parameters involves iterative procedures which employ an approach of modifying the parameters of an initial guessed model which are used to compute a new model response and the observation values is monitored. The model response can be either a linear or nonlinear function of the model parameters. The plot of apparent resistivity versus spacing is always a smooth curve where it is governed only by vertical variation in resistivity.

4.3 The Computer Program

The transfer of raw data to computer is important to do the process of reduction, inversion and analysis. Then the determination of the final model parameters will be done by using the computer program, Win-resist (Win-resist Version 5.1, 1981-2001). What is actually going on the program is briefly outlined below:

1. Type used in the data collection is specified and the field data for each sounding station is loaded along with the current electrode spacing. Thus, a measured resistivity values are displayed with error bars indicating the estimated accuracy. This is done for all sounding stations.
2. A skilled guess of layer parameters (which is based on a geological concept or obtained by curve matching) are fed to the computer as input into the computer. When choosing the model entering option, the program enquires for the number of layers, resistivity, and thickness assumed for the initial guess. The program requires the values to be given in order and starting from the first layer.-after the required inputs as specified above is supplied. The program displays the graph of the field curve with the model given in step above.
3. The apparent resistivity curve for the input model of step 2 is computed, using a forward calculation. This makes the program ready for comparison of the theoretical curve and the field curve.
4. Trial-and-error adjustments of the layer parameters are made until the theoretical computed curve agrees with the measured curve. And this iteration process continues as commanded by the user until the calculated error is within the prescribed error limit. By these process the resistivity and depth values of each VES is quantitatively determined. These parameters are used for construction of geo electric sections which indicate the electrical stratification of the studied

4.4 Inversion of Audio Magneto Telluric Data Set

In the previous chapter it shown that a 2D analysis is justified for the ziway -butajira and meki-mider kedbd AMT data set. Therefore, 2D inversion was applied to the data set to determine the subsurface resistivity structure .the larger evenly distribute ATM data set allows a 3-D inversion to be used to investigate the validity of the 2D approach.

4.4.1 Two Dimensional Magneto Telluric Inversion

Tensor decomposition and induction vector showed that ziway– Butajira and meki- miderkebd AMT data were relatively 2-D .Thus an initial approach was to use a standard 2D inversion to convert the fre9uency domain MT data in to a model with true depth on the vertical scale. Iterative linear inversion is the most widely used approach for solving nonlinear inverse problem of geophysics .in this approach, an initial resistivity models is generated and the predicted MT data are computed .the model sensitive are then computed and used to calculate a change in the resistivity model that will improve the fit to the measured MT data.

CHAPTER FIVE

DATA PRESENTATION AND INTERPRETATION

5.1 Pseudo depth Sections

One way of presenting the measured apparent resistivity values is in the form of pseudo sections along a profile, the field data, obtained from each sounding is gridded and displayed as regular contour maps, displaying areas of anomalously high or low, value, so pseudo sections are basically meant for qualitative interpretation and show the lateral and vertical variation of electrical properties, with in the sub-surface (Ewenetu Gashawbeza, 1998). In this thesis work the pseudo sections are constructed using mapping software called Surfer 10 (surfer 32-bit).

5.2 Apparent Resistivity Pseudo depth sections

5.2.1 Pseudo depth Section of Profile -1

This lines represents the south east part of the study area Ziway and Runs, nearly North west direction, It comprises six resistivity sounding points, namely VES-1, VES-2, , VES- -3 , VES-4,VES-5 and VES-6 they are positioned at horizontal distance of Om, 2685m, 8477m , 12024m,14483m and 16380m respectively ,beginning from the south eastern end of the line. The elevation of VES-1, and VES -2 are almost the same. [1662 & 1666 m.a.sl] VES-3, VES-5 and VES-6 also the same rises to (1814 to 1849 m.a.sl) and VES-4 is1769 m.a.sl. Fig 5.1 shows the general electrical picture of the ground section along line -1.High resistivity ranging from 140-300ohm-m is observed below VES -2 and VES-5, Resistivity ranging 20Ω-80 Ω are found below VES-3 & VES-4 and which is also visible below VES -2, VES-5 AND VES-6 at deeper depth below400m, low resistivity zone 120 Ω -160 Ω are located at the top of VES-1. From pseudo section profile-1 at the deeper depth there observed very less resistivity value ranging from 0Ω -80 Ω deep under VES-2,VES4 and VES-5This means that to the right of VES -2 [to North West direction], the resistivity value shows gradually decrement.

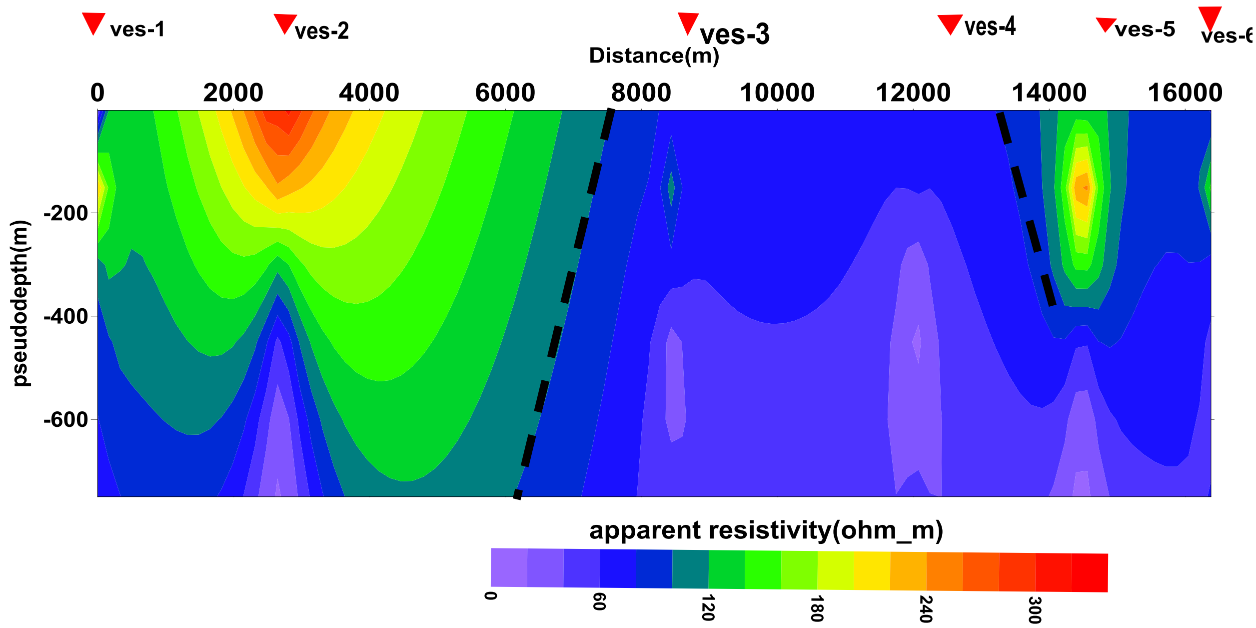

Figure 5.1 Apparent resistivity pseudo depth section along Profile 1, Ziway-Butajira traverse, Central Main Ethiopian Rift.

5.2.2 Pseudo depth Section of Profile – 2

This line runs over the south east part of the study area and across over in the direction of north south. there are seven resistivity sounding which are positioned at a distance of 20122m, 23940m,28244m,33120m,35557m,39481m,and42214m respectively from SE and Apparent resistivity pseudo section for this line is given:- in Fig. 5.2.As the pseudo section of Fig. 5.2 of this profile shows, the top layer around VES-11,VES-12 and VES-13 is relatively resistive compared to VES-7 ,VES -8, VES-9 and VES-10, low resistivity ranging from 0Ω-60 Ω m are found below VES-7, VES-8, VES-9 and VES-10.On pseudo section profile -2 low resistivity value below the depth 400m ranging 0-60 Ωm are observed under VES -12.Generally the resistivity decrease with increase depth and at deeper depth beneath VES-10 to VES-13 there exist very low resistivity zone. The pseudo section of profile-2 picture clearly shows that the direction of ground water flow from NW to SE direction and flow of Ground water from deeper depth of VES -11,VES-12 & VES -13 to the deeper aquifer. Beneath VES -7, VES-8 and VES-9...A discontinuities are observed on this survey line under beneath VES -11 which is 36km from starting point of the survey line.

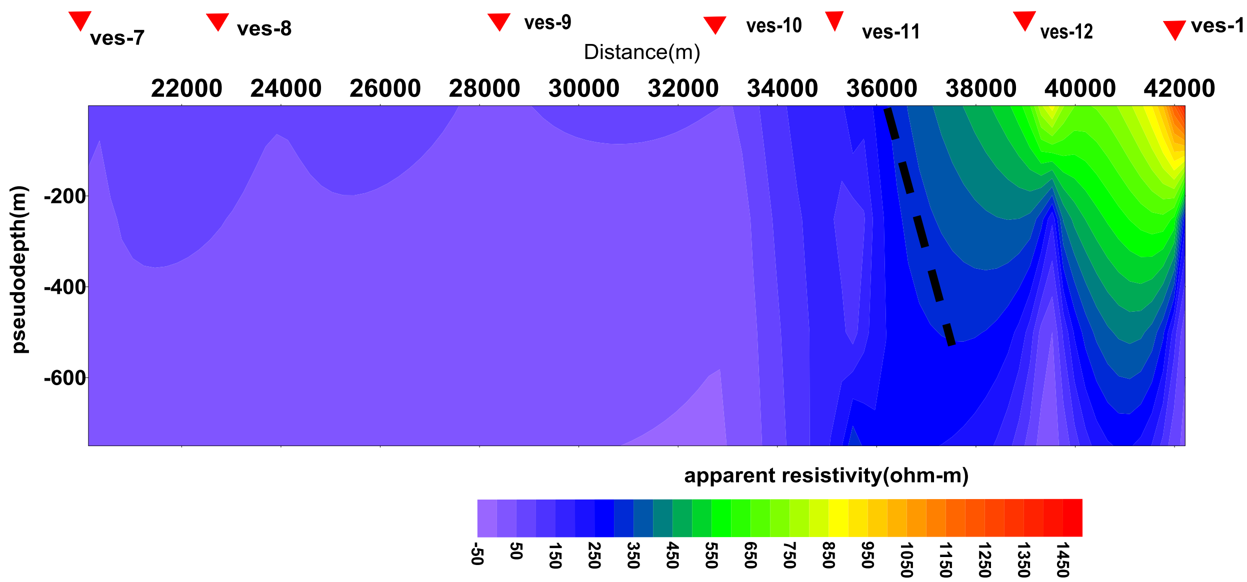

Figure 5.2 Apparent resistivity pseudo depth section along Profile 2, western side of Ziway- Butajira traverse, Central Ethiopian Rift.

5.2.3The Pseudo depth Section Profile-3

This lines represents the east part of the study area Meki and Runs nearly West direction of Dugda .It comprises five Resistivity Sounding points, namely, VES-1, VES-2, VES-3, VES-4 and VES-5 respectively they are positioned at a horizontal distance from east meki of 0m, 2971m, 6095m, 9369m and 13282m resistivity, and the elevation of VES-1 and VES-2 almost the same [1668masl and 1692 m.a.s.l respectively] and also the elevation of VES-3, VES-4 and VES-5 almost near to each other [1708masl, 1733masl and 1791masl respectively. Fig. 5.3 shows the general electrical picture of the ground section beneath profile According to the Fig5.3 generally low resistivity from 0Ω-200Ω m are observed at the top shallow depth beneath all VES- points from VES-1 to VES-5.High resistivity ranging from 1200Ω-3600Ω are found under ves-3. This shows there is a ground water flow from shallow depth of the Dugda to deep depth of eastern direction here along this profile two structures which are (8km) from the starting point are observed

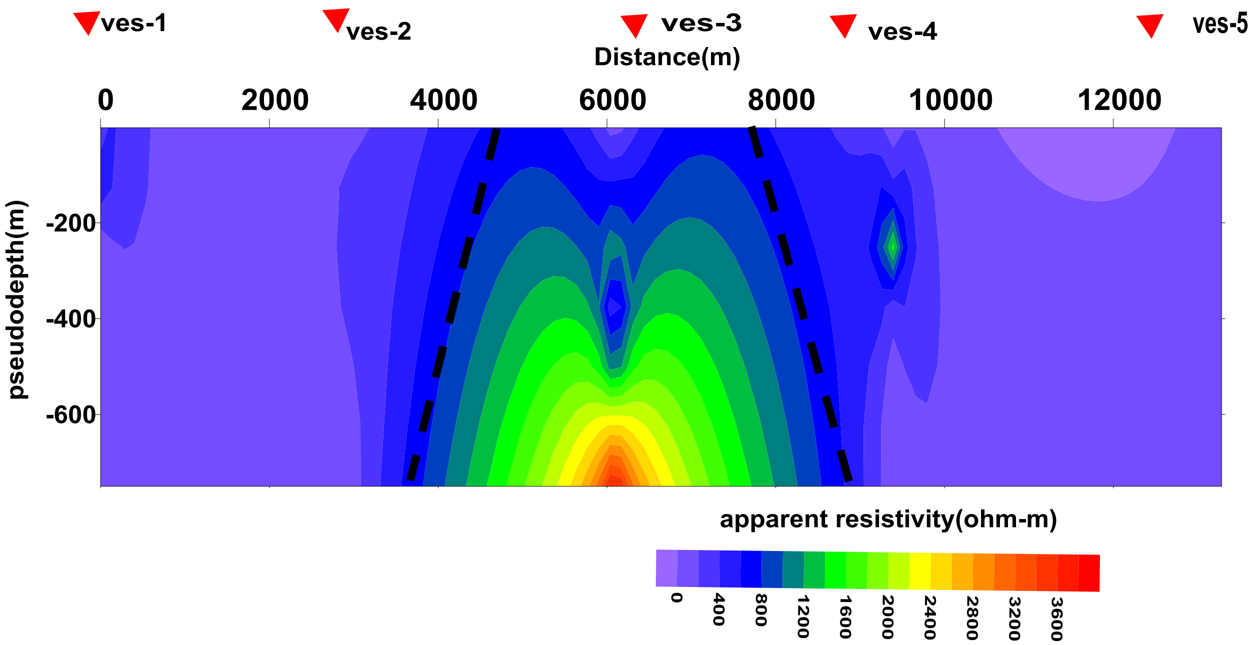

Figure 5.3 Apparent resistivity pseudodepth section, Meki-Dugda traverse, Central Main Ethiopian Rift.

5.2.4Pseudodepth Section Profile-4

This line runs over the south part of the study a dugdu Boru. A cross over in the direction of North to Midrekebd Escarpment. There are five resistivity sounding position at a distance of 17017m, 19758m, 22252m, 25990m and 28955 respectively from south end of Dugda Apparent resistivity of Pseudo section for this profile is given in Fig 5.4 As the Pseudo section of fig 5.4 of this profile shows the top layer shallow depth beneath VES-7, VES-8 VES-9 and VES-10 shows less resistivity ranging from 10Ω to 40Ω.There are observe thick layer relatively high resistive under VES- 6. Discontinuities are identified along this profile under beneath VES-7 which is 18km from the starting point of this profile.

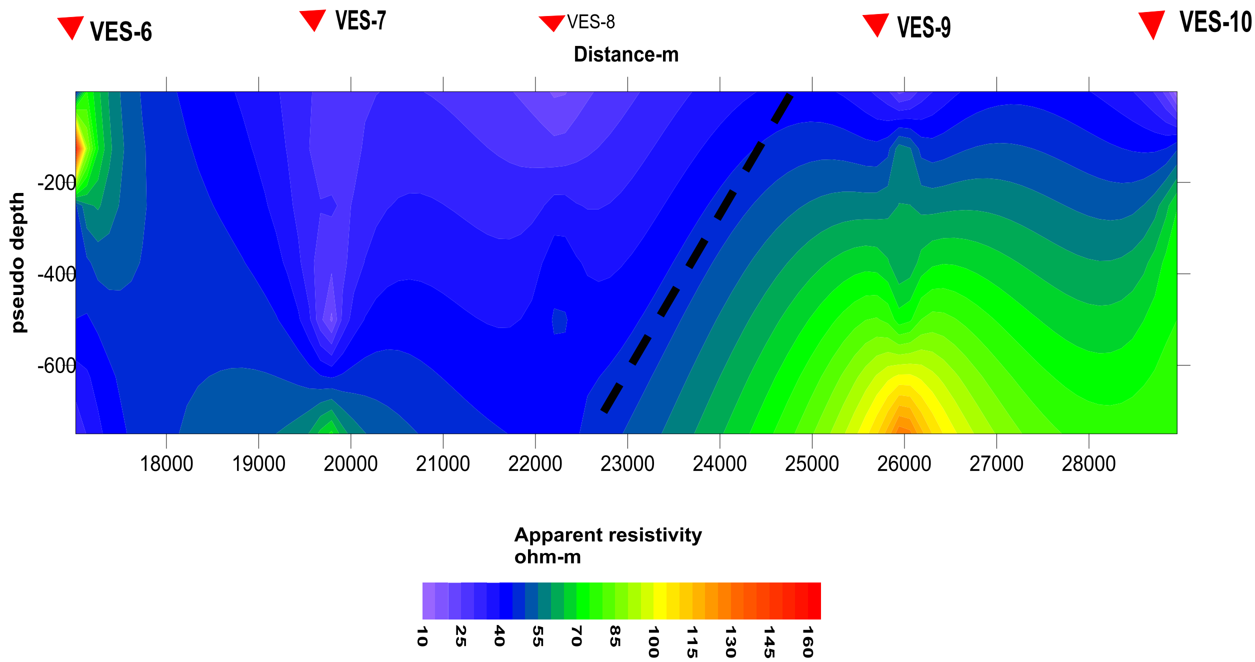

Figure 5.4 Apparent resistivity pseudodepth section along Profile 4, DugdaBoru - MidreKebd Traverse, Central main Ethiopian Rift.

5.3 Geoelectric Sections

5.3.1 Geolectric Section along Profile-1

From the interpreted layer parameters of VES-1 to VES-6 (Fig.5.5), the resistivity sounding geoelectrics section along line 1 is constructed. The dry soil is characterized by relatively high resistivity values as well as very resistive and this difference is believed to be due to variation of moisture Content .this layer has nearly 0.5-8m thickness, there some of the resistivity value of the top layer on (Fig.5.5) is somehow exaggerated. The second layer form a resistivity range of 12Ω-171Ω- m and thickness varying 1.6m to 26m beneath the VES points. This layer is inferred as highly fractured and weathered basalt. The next layer has 52Ω-120Ωm resistivity range which represent massive basalt under VES-2 and VES-5, this layer has a thickness of about 66m to 89m, from VES3 to VES6 which inferred by highly fractured and weathered basalt and thickness about 7.1m to 91.1m beneath VES-points. The last part of the cross section along line 1 is covered by the main aquifer in the area highly fractured and weathered ignimbrite. Having resistivity of 8Ω-34Ω m this low resistivity zone is believed to be a good means of ground water moister.

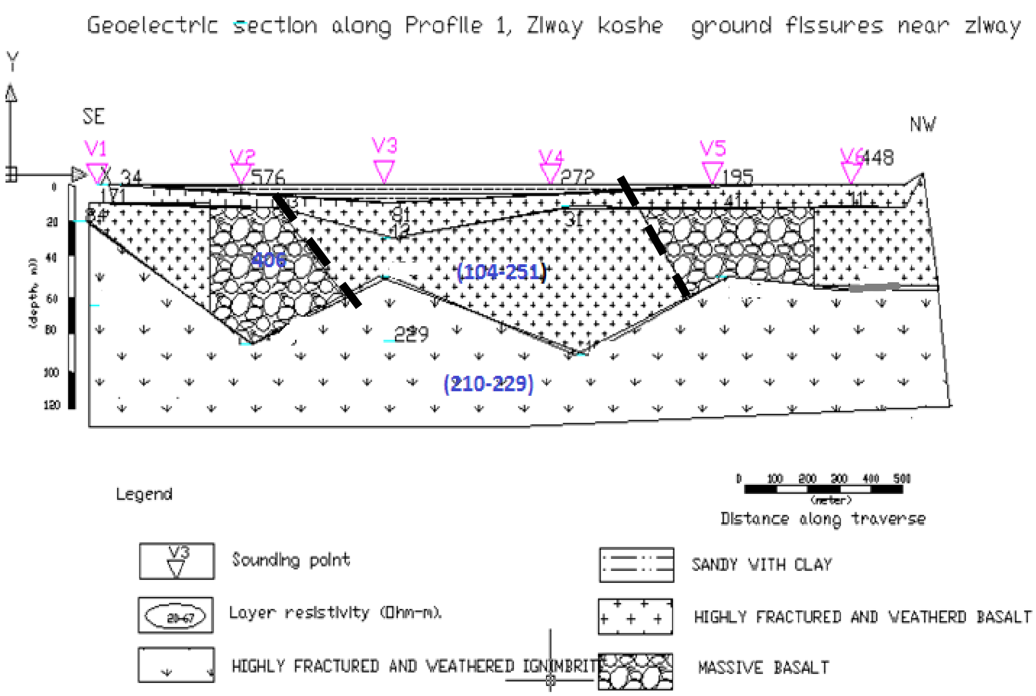

Figure 5.5 Geoelectric section Profile-1 around Koshe

5.3.2 Geoelectric section along Profile-2

From the interpreted layer parameter of VES-7 to VES-13 (Fig.5.6) along line, is consternated. The resistivity of the upper most layer ranges between 38Ω-1018Ω m which is clay with rock fragment and have thickness 0.5-0.9m, here also the top layer some of the resistivity value on (Figure 5.6) is somehow is exaggerated. Underlying the top-layer, beneath VES-7 to VES-13 the subsurface is characterized by low resistivity ranging from 11Ω-41Ωm and has average thickness 40.72m.Which represents highly weathered and fractured basalt. The third layer beneath VES-7 to VES-11 having resistivity 5.9Ω to 331Ω m which represents highly fractured and weathered basalt show large lateral variation in resistivity with respect to the layer beneath VES-11 and VES12 which has resistivity ranges 331Ω-2552Ωm Here the existing resistivity variation possibly shows the presence of contact. The last layer of cross section is found bellow an average depth of 206m, the resistivity varies from 5.6Ω-34Ω m and it may be attributed to possibly fluid saturated slightly weathered and fractured ignimbrite which is distributed over the area.

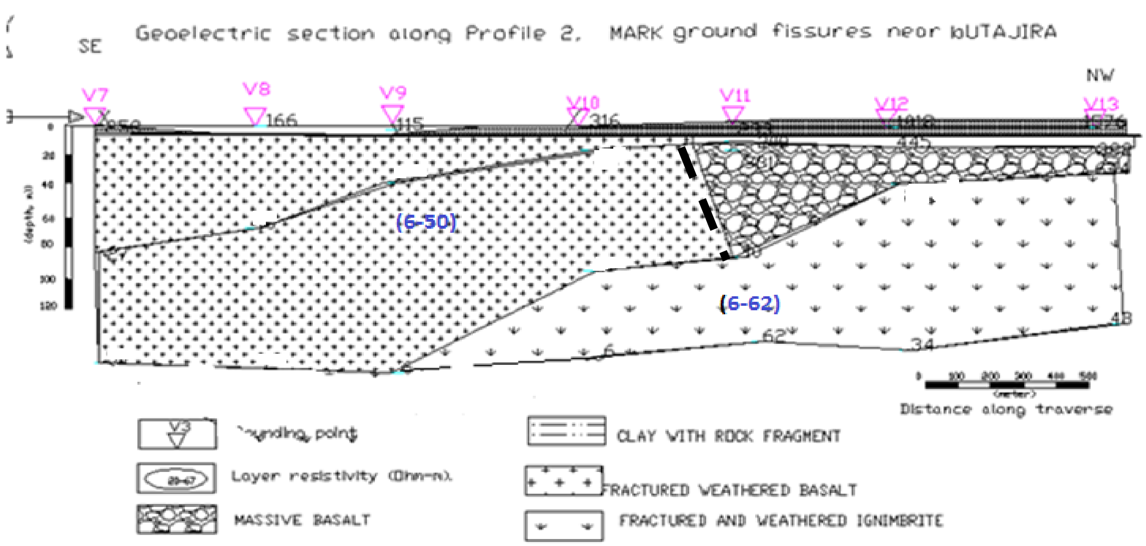

Figure5.6 Geoelectric section of Profile-2 around Marko Woreda near Butajira.

5.3.3 Geoelectric section along Profile-3

The resistivity sounding geo electric section along line -3 is constructed from the interpreted layer Parameters of VES 1 to VES-5 (Fig.5.7), it shows that beneath each point and the resulting geo electric section is presented (Fig5.7) shows VES-1, has four layer whereas VES-2, VRS-3, VES-4 and VES-5 have five layers respectively. The top most part of the cross section has resistivity value that range from 5Ω to 361Ω m , having thickens of about 0.7 to 12m, this layer is probably related to top layer, compacted fine grained sand Here some the resistivity value of the top layer, on(Fig.5.7) is somehow exaggerated. The second layer below the VES points has resistivity ranges 35Ω m to 241Ω m, there exist grained sand except that of grained pumice under beneath VES-3.The third layer except that of below VES1and VES-3 which is alluvial deposit has resistivity around 564Ω m with thickness 13m which is grained pumice. The resistivity value on the third layer below VES-1 somehow are exaggerated the fourth and fifth layer below VES-1 to VES-5 has resistivity 18 to 642 Ω m and has a thickness of 140m informs that the layer has covered by alluvial deposits.

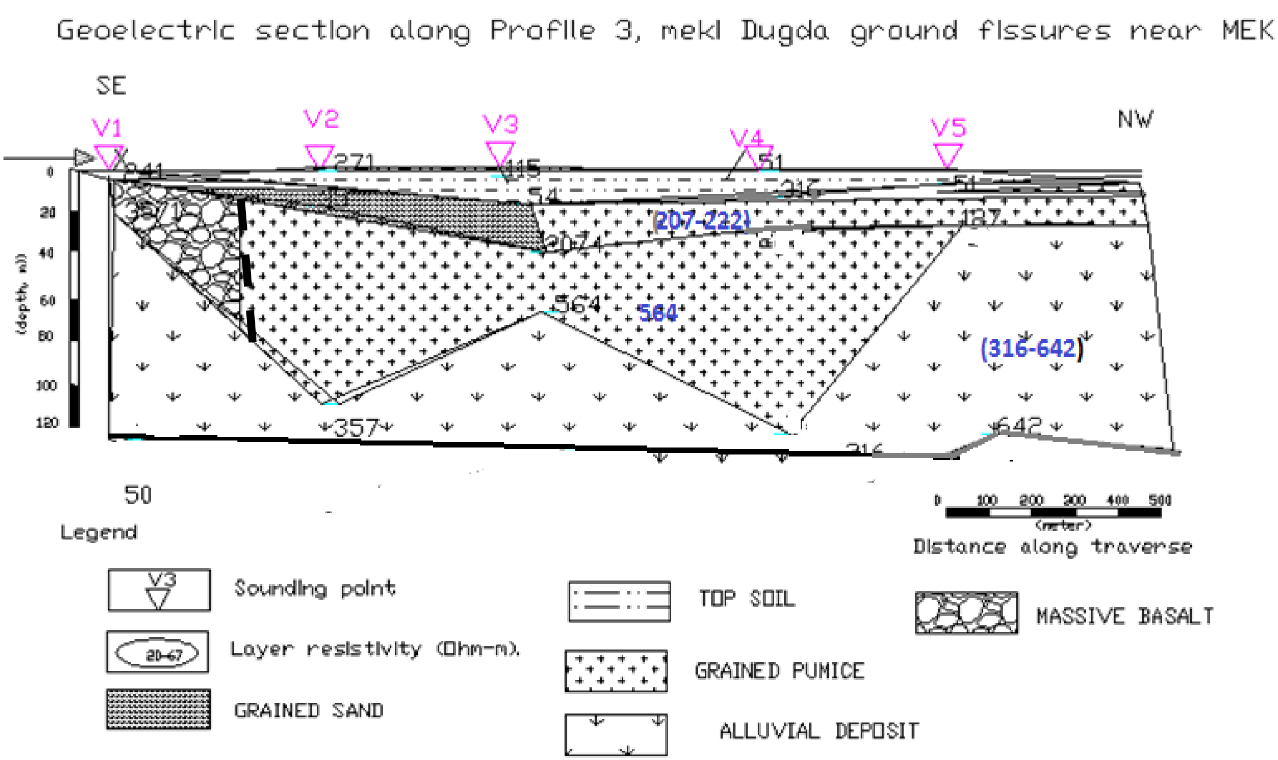

Figure 5.7 Geoelectric section along Profile-3, near Meki.

5.3.4 Geoelectric section along Profile-4

From the interpreted layer parameters of VES-6 to VES-10 (fig5.8), the resistivity sounding geo-electrics section along line 1 is constructed. The silt clay with sandy material is characterized by relatively low resistivity value ranging (7 Ω to 38Ω m) .this layer has nearly 1.1 to 5.8m thickness. The second layer form a resistivity range of 13Ω-58Ω m and thickness varying 1m to 294.2m beneath the VES points. The third layer under below VES-9 is inferred as highly fractured and weathered ignimbrite and under the other VES points (VES6, VES7, VES8 and VES10) which is filled by fine grand sand with some pyroclastic materials. The last layer has 8Ω-244Ω m resistivity range which represent moderately welded weathered tuff under beneath VES6,VES7 and VES-8, VES9 to VES10 which inferred by highly fractured and weathered tuff and thickness about 75.4m to 294.2m beneath the VES points. The last part of the cross section along line 4 is covered by the main aquifer in the area moderately fractured and weathered tuff. With this low resistivity zone is believed to be a good means of ground water movement.

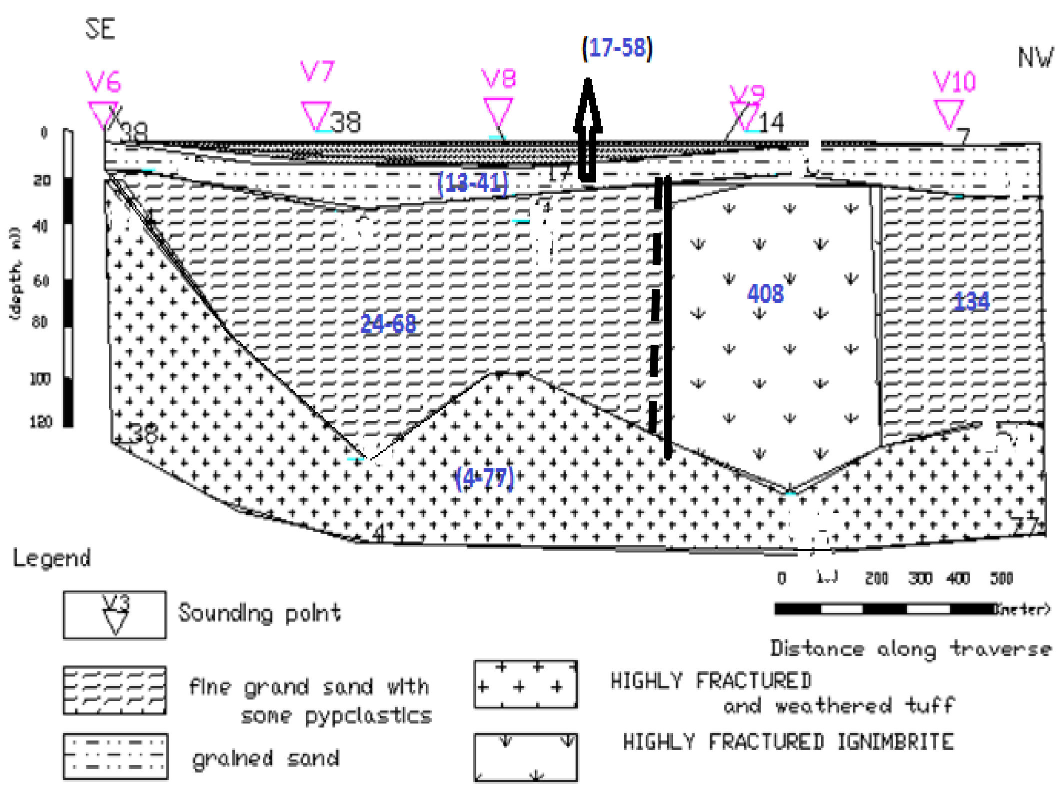

Figure 5.8 Geoelectric section along Profile-4 near to MidreKebd.

5.4 2D Magneto telluric Geoelectric Sections

5.4.1 2D MT section along Profile -1

According to the 2D MT resistive section (Figure 5.9) a clear picture of the subsurface is mapped at a great depth over 1000m. The upper most layer under beneath MT1 and MT2 and beneath MT4 and MT5 characterize by relatively low resistivity less than 10 Ω represented by cyan and blue in color. Which is related to comprise the clay with rock fragment and highly fractured and weathered ignimbrite having thickness from 200m to 300m. The top most layer under beneath MT3 represented by yellowish color having relatively high resistivity value greater than 14 Ω which may correspond to massive basalt. Underlying the basaltic rock a layer represented by yellowish color may mapped which is interpreted to consists of massive basalt thicker and deep in south eastern part and getting thinner and shallow towards north west of the traverse.

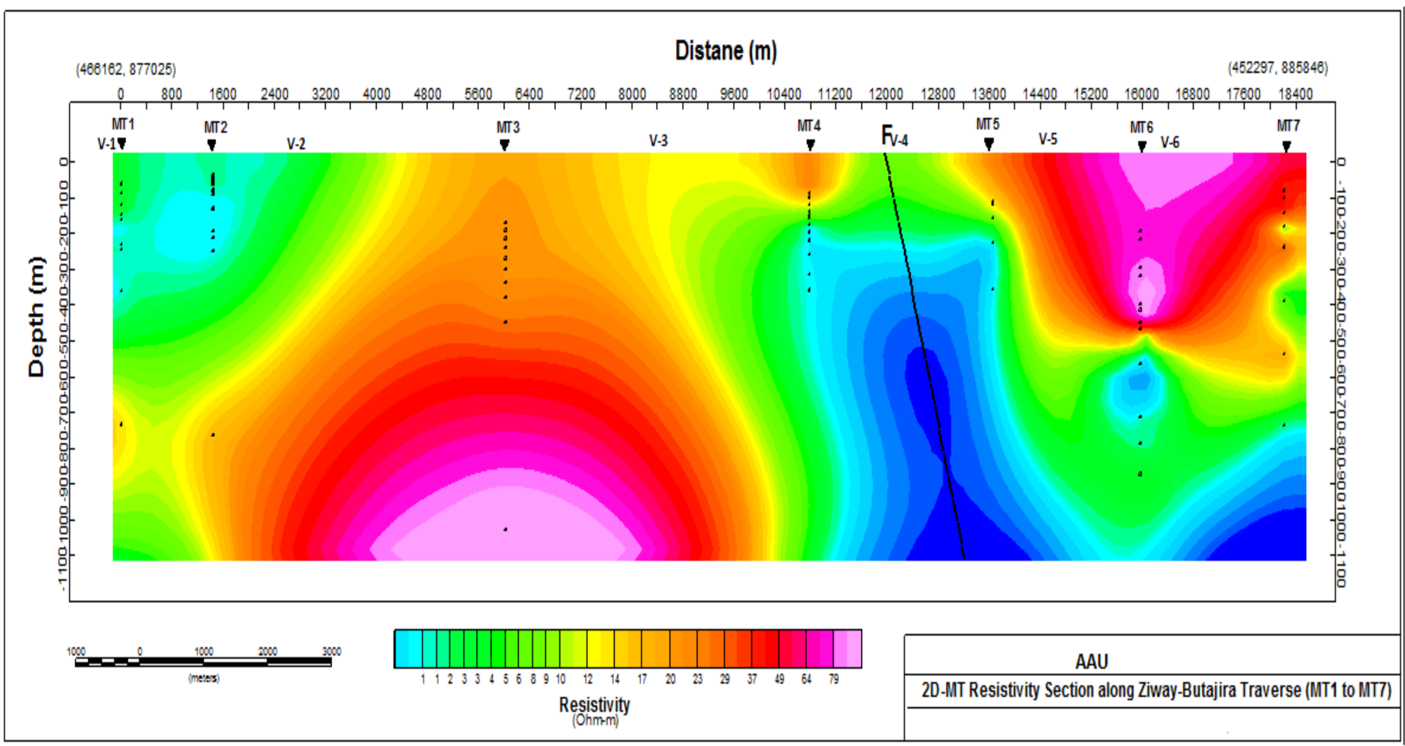

Figure 5.9 2D AMT section along the eastern part of Ziway- Butajira Traverse, Central Main Ethiopian Rift.

The substratum which is represented by red in color on the 2D MT resistivity section (Fig.5.9) could have associated with basement rock of moderately fractured weathered rhyolite .this rock unit is getting shallower as one goes from MT1 to MT7 ,which means the basement is deeper beneath MT3 and shallower beneath MT6 and MT7 observation point ta discontinuities are identified on this 2D MT resistivity profile -1 the most noticeable is being that observed at 12km from starting point of this profile beneath between MT4 and MT-5 which is more than 1000m in depth. In general as per the objectives of the present survey, by low fre9uency MT method it was possible to penetrate deeper greater than 1000m and able to map the moderately fractured and weathered rhyolites which is considered as high productive aquifer.

5.4.22D MT Geo electric section along Profile -2

The 2D MT resistivity geo electric section along profile -2 (Fig5.10)discussed the top most part of the cross section beneath under MT8 and from MT10 to MT13 which represented by relatively low resistivity less than 4 Ω identified by green color related to clay with rock fragment and highly fractured and weathered ignimbrite having thickness from 100m to 300m.The upper most layer under beneath MT9 represented by red color having relatively high resistivity value greater than 14Ω which may represents highly fractured and weathered basalt. allayer represents by red color was mapped which is related to highly fractured and weathered basalt it is deep thicker towards south east under beneath MT8 and MT9.on the other hand which is deep and thinner towards north west under beneath MT12 and MT13.In the central part of the geo electric section under beneath between MT10 and MT12 the resistivity value ranges from 6Ω to 7 Ω are observed which may also considered as high conductive deep a9uifer of highly fractured and weathered ignimbrite .in this 2D MT profile no discontinuities are observed.

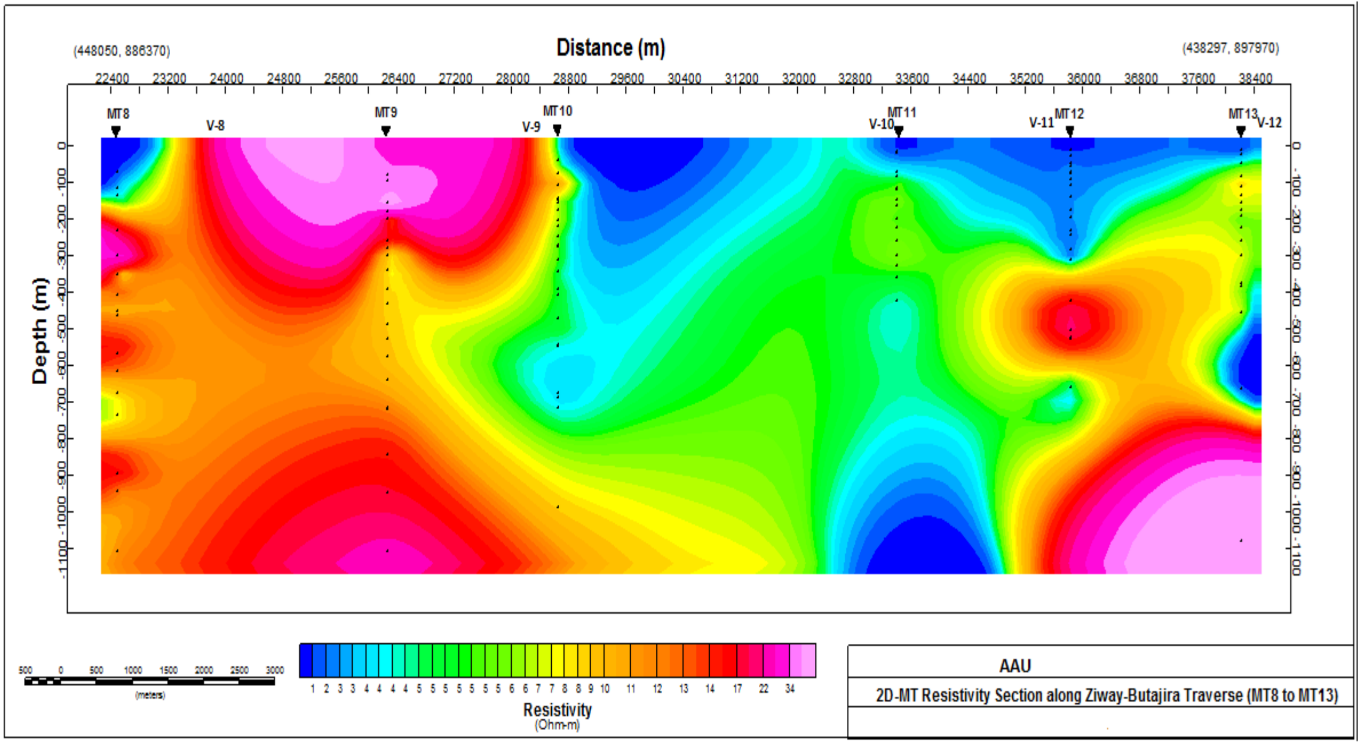

Figure 5.10 2D AMT section along Ziway - Butajira traverse, western side, Central Main Ethiopian Rift.

5.4.3 2D MT Geoelectric Section along Profile -3

According to the 2D MT resistivity section (Fig.5.11) the upper most layer under beneath MT1 and MT7 there observed relatively low resistivity ranging from 1Ω ohm to 4 Ω this section is characterize by green color which represents grained sand and grained pumice having thickness 100m to 200m.The top most layer depth (out of MT1 and MT7) up to 300m represents relatively also low resistivity value not greater than 7Ω this section may corresponds to grained pumice .under laying the grained pumice a layer represented by yellowish and red color was mapped which is interpreted to consists of alluvial deposit, thicker and deep under beneath MT3 and also thicker wide and deep under beneath from MT5 to MT8 towards north west direction of the traverse .in this 2D MT resistivity Profile -3 from Meki to Dugda Boru at least three discontinuities are observed the first one 2.4 km from the starting point of this profile, this structure is clearly visible in the area of our survey, which is between MT2and MT3 and assumed to be continued more than 1200m in depth.

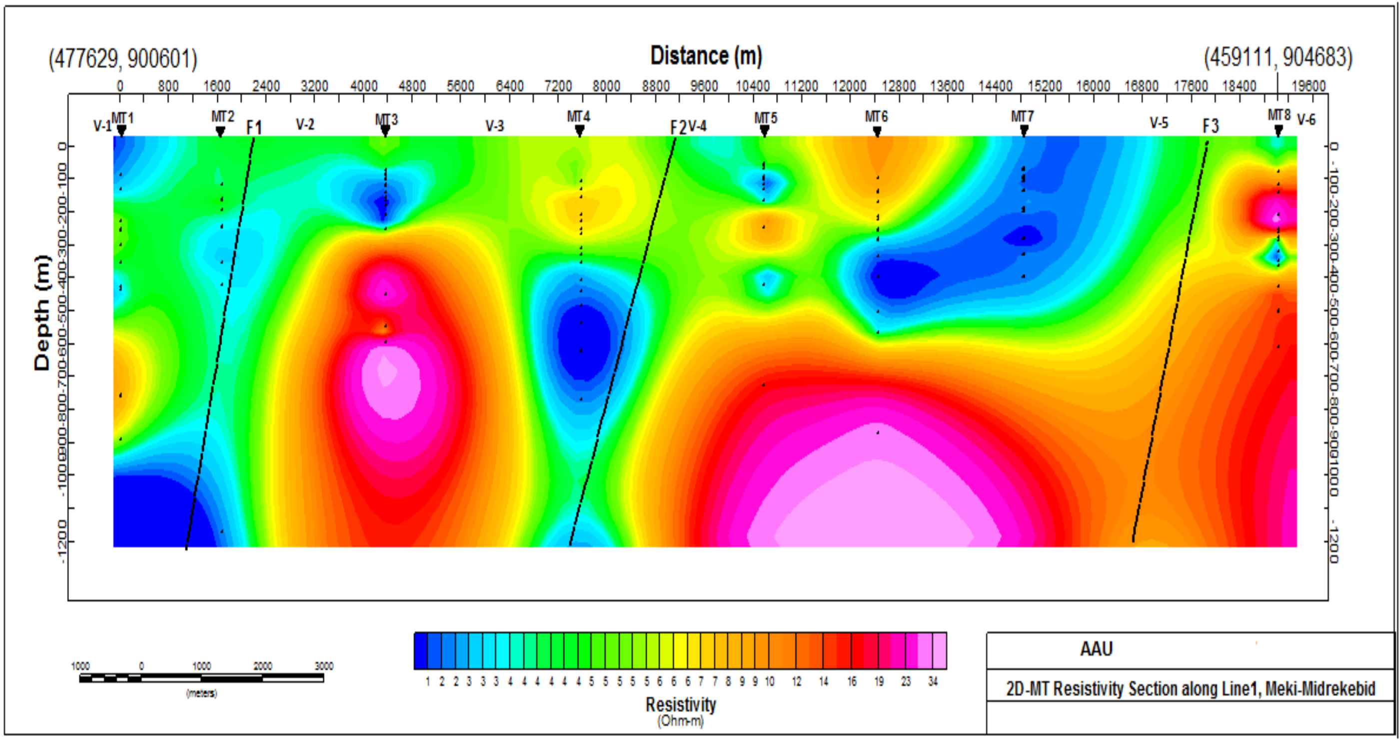

Figure 5.3 2D MT section along Meki-MidreKebd traverse eastern side, Central Main Ethiopian Rift.

The second dis continuity is 9km far from the starting point of this profile it is between MT4 and MT5 which is more than 1200m in depth .the third discontinuities is between MT7 and MT8 which is 18km from the starting point of this profile in depth is similar to the others which is more than 1200m in depth.

5.4.4 2D MT Geoelectric section Profile-4

This line runs over the south part of the study area Dugda Boru across over in the direction north to MidreKebd escarpment. In (Fig.5.12) The upper most layer under beneath between MT8 and MT9, in addition under beneath MT11 and MT12 relatively observed less resistivity ranging from 1Ω to 4Ω and thicker 300m to 400m this section is represented by green color it is the shallow depth less resistivity value corresponds to welded weathered tuff and fine grained sand with some pyroclastic materials.

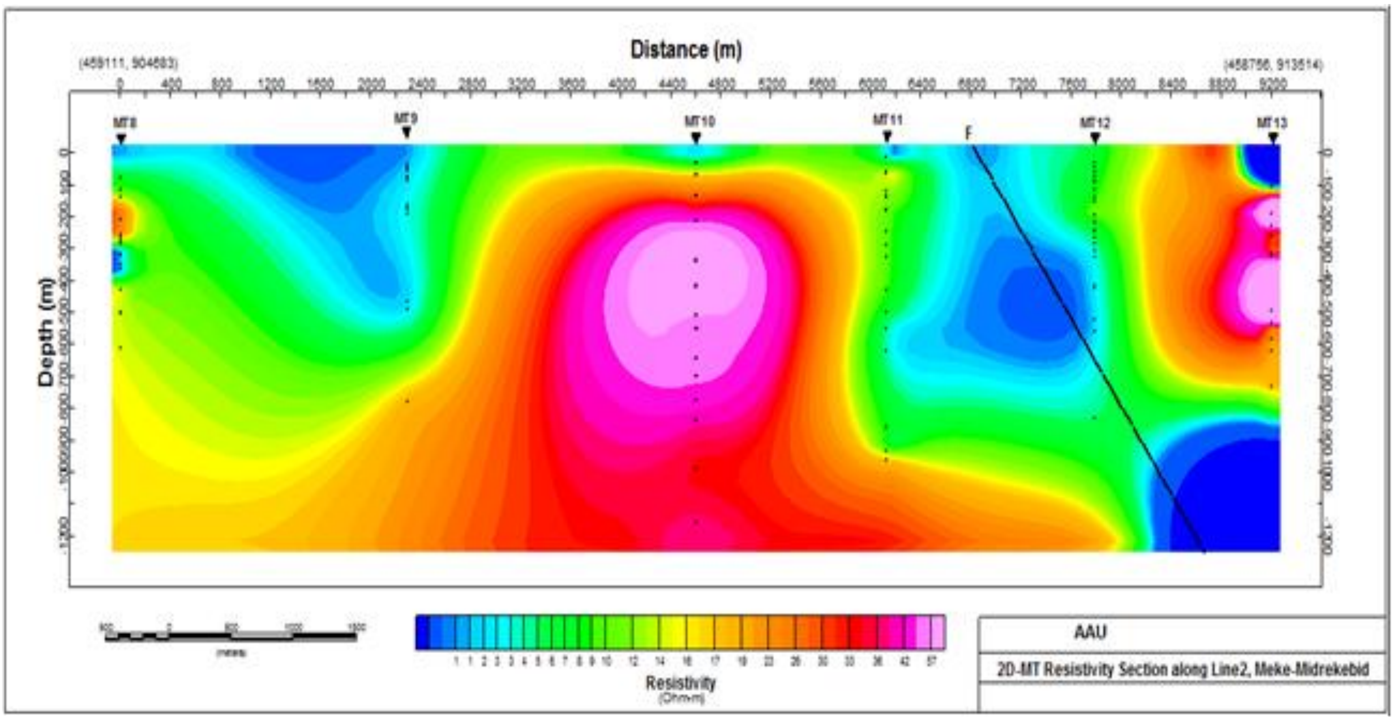

Figure 5.4 2D MT section along Meki MidreKebd traverse south north direction of Central Main Ethiopian rift.

The top most layer at under beneath MT10, MT12 and MT13 represented by yellowish color having relatively high resistivity value greater than 16Ω which may corresponds to moderately fractured ignimbrite. This moderately fractured ignimbrite rock a layer represented by yellowish red color is deep thicker and wide under beneath MT10 in the center of the traverse along profile line 4, thinner and shallow under beneath MT13 The sub stratum which is represented by 2D MT resistivity ranging from 6 Ω to 14Ω which may represent by fine grained sand with pyroclastic material this rock is thicker and shallow as one goes from MT8 to MT9 and MT11 MT13 towards the northern direction of the traverse.

CHAPTER 6

Conclusions and Recommendations

6.1 Conclusions

The hydrogeological situation of the area has been inferred by comparison with the resistivity sounding and AMT along with the available geological and borehole information. Based on the work done in the current work and existing ones it was possible to make the following concluding remarks:

- For practical reasons it is easy and inexpensive to obtain direct current resistivity data using VES to explore the shallow depth but difficult and expensive to obtain deeper data and detailed structure for depth of hundred meters and more. Yet the MT data are better interpreted with knowledge of shallow condition provided by the VES method as shown in the present study and hence, the combination of VES and AMT methods providing an efficient geophysical tool for deep hydrological investigation.

- The apparent resistivity pseudodepth sections and the true resistivity geoelectrical section constructed from the VES data showed the presence of shallow and deep low resistivity horizons which could have most likely resulted from groundwater saturation.

- The MT surveys have mapped areas of low resistivity response at various locations (to depths of up to 1100 m) along the traverses that could have most likely resulted from subsurface water saturation.

  Near vertical geological structures have been inferred in particular along the geoelectrical profiles one, three and four; and these structures are taken as pathways for groundwater flow from shallow to deeper horizons..

- Along Ziway-Butajira and Meki-MidreKebd traverses, shallow and deep groundwater flow system have been identified from the resistivity data analysis: the shallow groundwater system formed up to 250m depth while the deeper groundwater system are formed below 250m up to 1000m and will continue in-depth as confirmed from VES and AMT data analysis. From the structures mapped with the survey and their vertical extent, it is clear that there is an interflow between these depths.

6. 2 Recommendation

- The aquifer system of the area is controlled by the structural lines and the basement topography so that drilling is recommended to be done at places having low resistivity responses that continue in depth. The structural features such as fault discontinuities are encountered in highly weathered and fractured basalt and ignimbrite or alluvial deposits.

- Based on the AMT and VES data analysis, the following locations are recommended for drilling to minimize the scarcity of drinking water around the study area. The preferred areas are in the following order. The first borehole is recommended along Ziway-Butajira traverse Galorepi Kebele VES-4 (between MT4 and MT5) around 12km from starting point of profile one, the second recommended borehole is also along Ziway Butajira traverse Batile Kebele VES-10 (MT11) which is 32km from starting point of prfile-1 with UTM (457903E 884101N)and (441082E 894395N) respectively and the others recommended borehalls along Meki Miderkebd travesrse are Girba Kebele VES-2 (MT2) which is 2.4km from Meki and Soloke kebele which is 25.8km from Meki VES-9(B/N MT11 and MT12) with UTM(474829E 901242N) and (459561E 910631N) respectively

- Similar detailed gravity and magnetic survey over the area, along the transects and over distributed points adjoining them is recommended to know the extension of faults structures that are believed to serve as conduits for groundwater flow and to study the extension of the promising low gravity and low resistivity zone in the shallow and deeper case ground water flow system.

- No definite correlation could be made between the fluoride concentration and the saturated zones and/or structures. Further hydrological and especially hydrochemical investigations are recommended to understand the implication the shallow and deep groundwater saturated zones and the major structures in relation to fluoride concentration.

REFERENCES

1. Abebe T. et al, 2005 Geological map of northern main Ethiopia rift (AG Consult, 2008, Butajira –Zuway area development study project.
2. Abiyu kebede (2008) . Unpublished M.Sc. Thesis Addis Ababa University, Ethiopia,
3. Aynalem Ali (1985). Hydrology of Addis Ababa. Unpublished M.Sc. Thesis Addis Ababa University, Ethiopia,.
4. B. Abebe et al, 2007, Quaternary faulting and volcanism in the main Ethiopia rift
5. Berhanu Gizaw (1996). The origin of high bicarbonate and fluoride concentrations inWaters of the Main Ethiopian Rift Valley, East African Rift system. *J. Afr. EarthSci*. **22**(4):391–402.
6. Boccaletti, M., Getaneh, A., Tortorici, L., (1992). The Main Ethiopian Rift: an example of oblique rifting. *Ann. Tectonicae,* **6**, 20–25.
7. Brooks, L. E. and Masson, J. L. (2005). Hydrology and simulation of ground water floIn Cedar valley, Iron County, Utah: U.S. Geological Survey, Scientific Investigation Report 2005-5170, 114 p.
8. Butajira- Ziway Area development study, AG Consult Consulting Hydro geologists & Engineers Plc., 2008.
9. Caroline L., Jean-Jacques T, Elisabeth G, Yves T, Kiram L, Jean R, Marc M, Raymonde B,Michel D, Bernard G, Vincent J, Endale T, Mohammed U., Balemwal A.,Tesfaye C., David W, Maurice T, (1999). The Ziway–Shala lake basin system, Main Rift
10. Chorowicevet (2005), East Africa rift system (EARS)
11. Christine Vallet-Coulomb and et al, 2001. Lake evaporation estimates in tropical Africa (Lake Ziway, Ethiopia). Journal of Hydrology 245 (2001) 1-18.
12. Dagnachew Legesse, 2002. Analysis of the Hydrological response of the Ziway Shala lake basin (Main Ethiopian rift) to change in climate and Human activities PHD thesis, AIX-en– provincie, France, Universitied AIX- Marselle III
13. Ewunetu Gashewubeza. (1998) Application Electrical resistivity and Electromagnetic prospecting method for ground studies around dembi, near Debrezieit . Unpublished Msc thesis Addis Ababa University, Ethiopia.

14. Eyasu Bunaro., (1998).Application of resistivity methods for ground water exploration around Chuko, southern region of Ethiopia. Unpublished M.Sc. Thesis Addis Ababa University, Ethiopia.

15. Gediy, W., Et al. (1990). Geology , geochronology and rift basin development in rthe central sector the main Ethiopian Rift Bull.Geol.Soc.America,

16. Hydrogeology and underground water modeling (Ministry of Water Resources and Water Technology Center, 2008).

17. Kazmin V, 1979 Stratigraphy and correlation of volcanic rocks in Ethiopia.

18. Kazmin, V.and Habtemecheal Berhe, S.1978.Geology and development of the Nazareth area. Ethiopian institute of geological survey.

19. Kifle Damtew, (1990). Geophysical investigation for construction material deposit in the Legedadi area. Hydrogeology journal Ethiopian Institute of Geological Survey (EIGS).

20. Mohr P., Zannetineb., 1988. The Ethiopian flood basalt province in MACDOUGALLJ.B (ED). Continental Flood basalt.

21. Mohr;P.A, (1967a). The Ethipoian rift system; Bull. Geophysical obs. Addis Ababa, No.II.

22. Orellana, E. and Mooney, H.M. (1966). Master tables and curves for Vertical Electrical Sounding over layered structures, *Interciencia*, Madrid.

23. Otto.k. (1879) Geosounding principles, I: resistivity sounding measurements ELSEVIER. Amsterdam.

24. Seifu kebede (2005). Ground water recharge, circulation and geochemical evaluation in the source region of the Blue Nile River, Ethiopia. Journal of Applied Geochemistry 10.1016.

25. Smith, J. T., J. R. Booker, 1991. Rapid relaxation inversion of two- and three-dimensional magneto telluric data, *Journal of Geophysical Research*, **96**, 3905 – 3922.

26. Solomon Tale (2000). The extent of surface water and ground water pollution. Unpub. MSc thesis, Addis Ababa University, 135 pp.

27. Tamiru Alemayehu (2006). Hydrogeochemical and lake level changes in the Ethiopian Rift. *Journal of Hydrology*. Vol **14902** VEERA—150762–. 1–11 pp.

28. Tekelehymanot R, Fikadu A., Bushra B. (1987). Endemic fluorosis in the Ethiopia rift vally. Tropical and geographythical medicine;

29. Tenalem Ayenew (1998). The hydrogeological system of the Lake District basin, Central Main Ethiopian Rift. PhD thesis, Free University of Amsterdam, 259 pp.

30. Tenalem Ayenew (2001). Numerical groundwater flow modeling of the central Main Ethiopian Rift lakes basin. SINET: Ethiop. J. Sci. 24(2):167–184.

31. Tenalem Ayenew (2005). Major ions composition of the ground and surface water sytems and their geological and geochemical and nuclear chemistry.

32. Tesfaye Chernet,travi,y.and Valles, V. (2001). Mechanism of degradation of the quality of natural water in the lakes region of the Ethiopian Rift Valley.

33. Tesfaye Chernet. (1982). Hydrogeology of the Lakes Region, Ethiopia (Lake Ziway, Langano, Abyata, Shalla and Awasa), Ministry of Mines and Energy, Ethiopian Institute of Geological surveys.

34. Tikhonov A. N. and V. Y. Arsenin, 1977. Solutions of ill-posed problems. V. H.

35. WHO (1984); Guidelines for drinking water quality 1st edn; Vol. I; Geneva; PP, 53.

36. Zohdy, A.A.R. (1989). A new method for the automatic interpretation of Schlumberger and Wenner Sounding curves.

Appendix

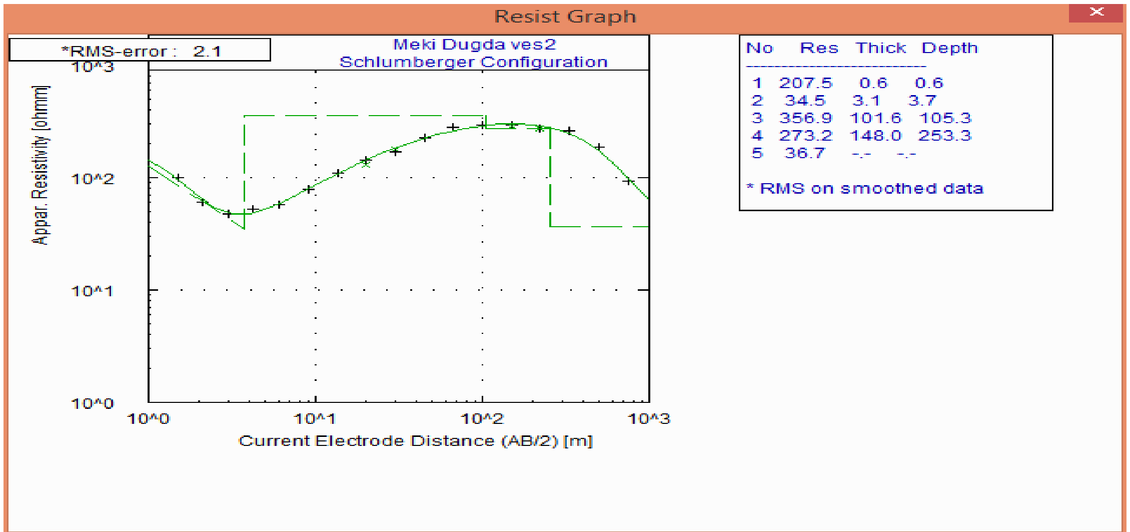
Resist Graph
*RMS-error : 2.1
Meki Dugda ves2
Schlumberger Configuration
Appar. Resistivity [ohmm]
10^3
10^2
10^1
10^0
10^0
10^1
10^2
10^3
Current Electrode Distance (AB/2) [m]
No Res Thick Depth
1 207.5 0.6 0.6
2 34.5 3.1 3.7
3 356.9 101.6 105.3
4 273.2 148.0 253.3
5 36.7 -.- -.-
* RMS on smoothed data

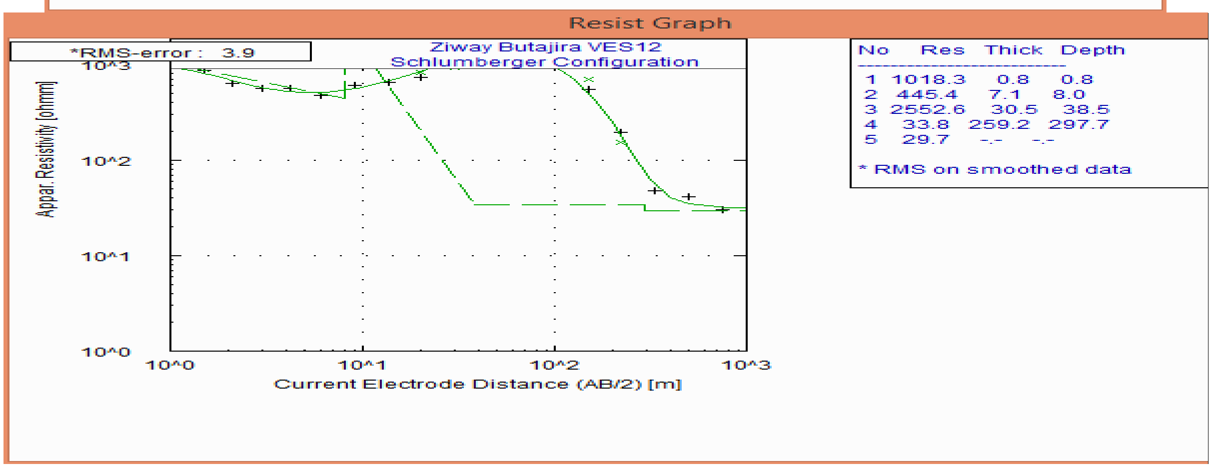
Resist Graph
*RMS-error : 3.9
Ziway Butajira VES12
Schlumberger Configuration
Appar. Resistivity [ohmm]
10^3
10^2
10^1
10^0
10^0
10^1
10^2
10^3
Current Electrode Distance (AB/2) [m]
No Res Thick Depth
1 1018.3 0.8 0.8
2 445.4 7.1 8.0
3 2552.6 30.5 38.5
4 33.8 259.2 297.7
5 29.7 -.- -.-
* RMS on smoothed data

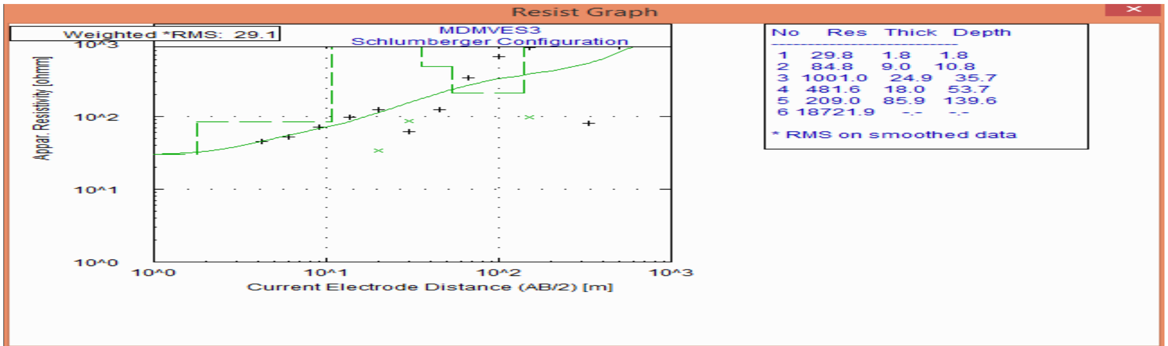
Resist Graph
Weighted *RMS: 29.1
MDMVES3
Schlumberger Configuration
Appar. Resistivity [ohmm]
10^3
10^2
10^1
10^0
10^0
10^1
10^2
10^3
Current Electrode Distance (AB/2) [m]
No Res Thick Depth
1 29.8 1.8 1.8
2 84.8 9.0 10.8
3 1001.0 24.9 35.7
4 481.6 18.0 53.7
5 209.0 85.9 139.6
6 18721.9 -.- -.-
* RMS on smoothed data

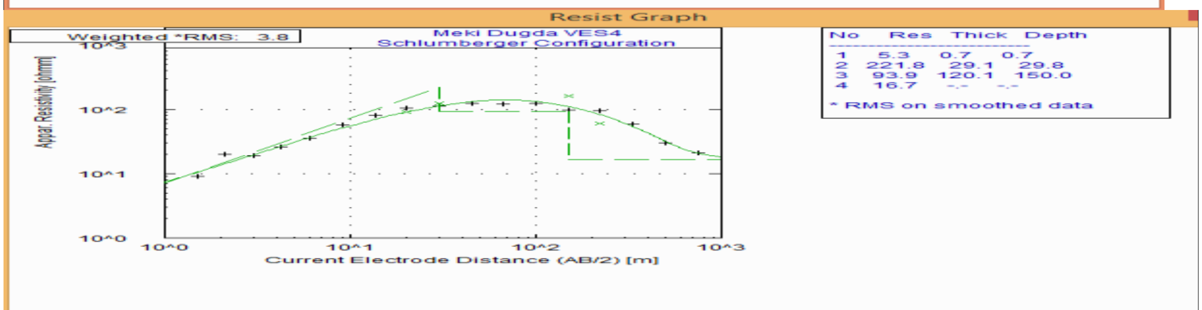
Resist Graph
Weighted *RMS: 3.8
Meki Dugda VES4
Schlumberger Configuration
Appar. Resistivity [ohmm]
10^3
10^2
10^1
10^0
10^0
10^1
10^2
10^3
Current Electrode Distance (AB/2) [m]
No Res Thick Depth
1 5.3 0.7 0.7
2 221.8 29.1 29.8
3 93.9 120.1 150.0
4 16.7 -.- -.-
* RMS on smoothed data

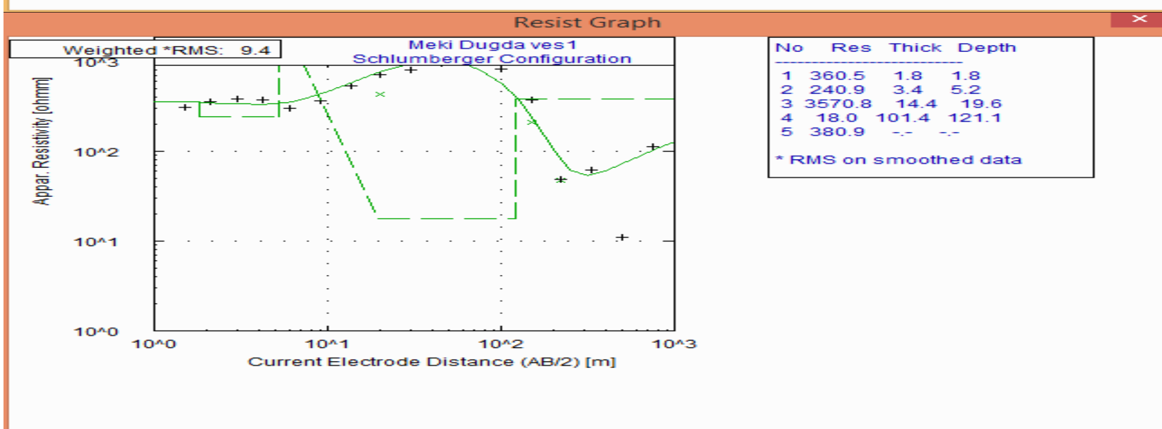
Resist Graph
Weighted *RMS: 9.4
Meki Dugda ves1
Schlumberger Configuration
Appar. Resistivity [ohmm]
10^3
10^2
10^1
10^0
10^0
10^1
10^2
10^3
Current Electrode Distance (AB/2) [m]
No Res Thick Depth
1 360.5 1.8 1.8
2 240.9 3.4 5.2
3 3570.8 14.4 19.6
4 18.0 101.4 121.1
5 380.9 -.- -.-
* RMS on smoothed data

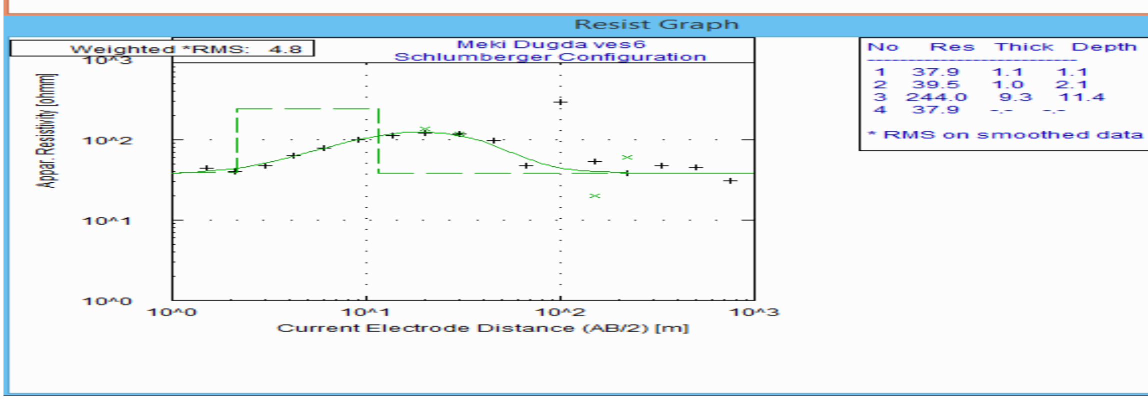
Resist Graph
Weighted *RMS: 4.8
Meki Dugda ves6
Schlumberger Configuration
Appar. Resistivity [ohmm]
10^3
10^2
10^1
10^0
10^0
10^1
10^2
10^3
Current Electrode Distance (AB/2) [m]
No Res Thick Depth
1 37.9 1.1 1.1
2 39.5 1.0 2.1
3 244.0 9.3 11.4
4 37.9 -.- -.-
* RMS on smoothed data

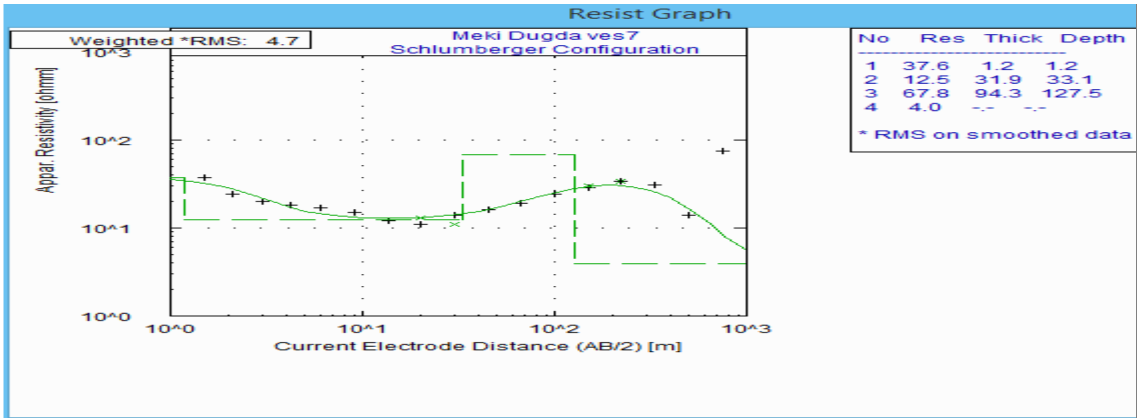
Resist Graph
Weighted *RMS: 4.7
Meki Dugda ves7
Schlumberger Configuration
Appar. Resistivity [ohmm]
10^3
10^2
10^1
10^0
10^0
10^1
10^2
10^3
Current Electrode Distance (AB/2) [m]
No Res Thick Depth
1 37.6 1.2 1.2
2 12.5 31.9 33.1
3 67.8 94.3 127.5
4 4.0 -.- -.-
* RMS on smoothed data

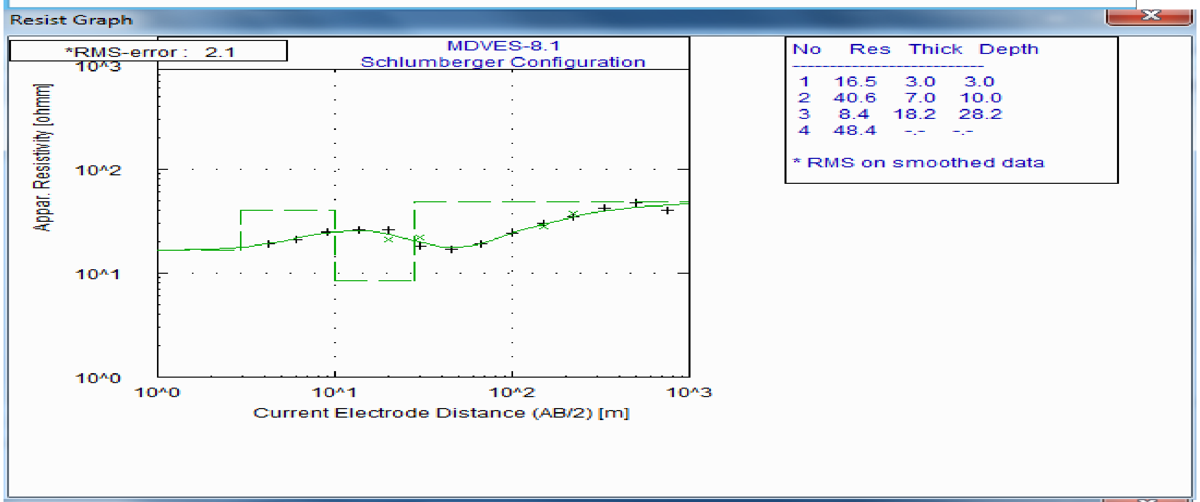
Resist Graph
*RMS-error : 2.1
MDVES-8.1
Schlumberger Configuration
Appar. Resistivity [ohmm]
10^3
10^2
10^1
10^0
10^0
10^1
10^2
10^3
Current Electrode Distance (AB/2) [m]
No Res Thick Depth
1 16.5 3.0 3.0
2 40.6 7.0 10.0
3 8.4 18.2 28.2
4 48.4 -.- -.-
* RMS on smoothed data

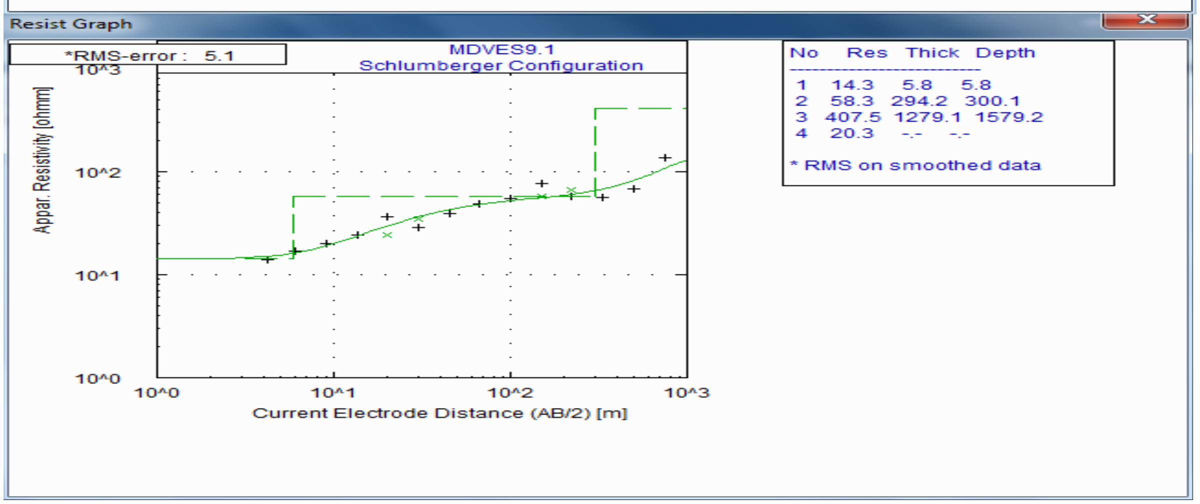
Resist Graph
*RMS-error : 5.1
MDVES9.1
Schlumberger Configuration
Appar. Resistivity [ohmm]
10^3
10^2
10^1
10^0
10^0
10^1
10^2
10^3
Current Electrode Distance (AB/2) [m]
No Res Thick Depth
1 14.3 5.8 5.8
2 58.3 294.2 300.1
3 407.5 1279.1 1579.2
4 20.3 -.- -.-
* RMS on smoothed data

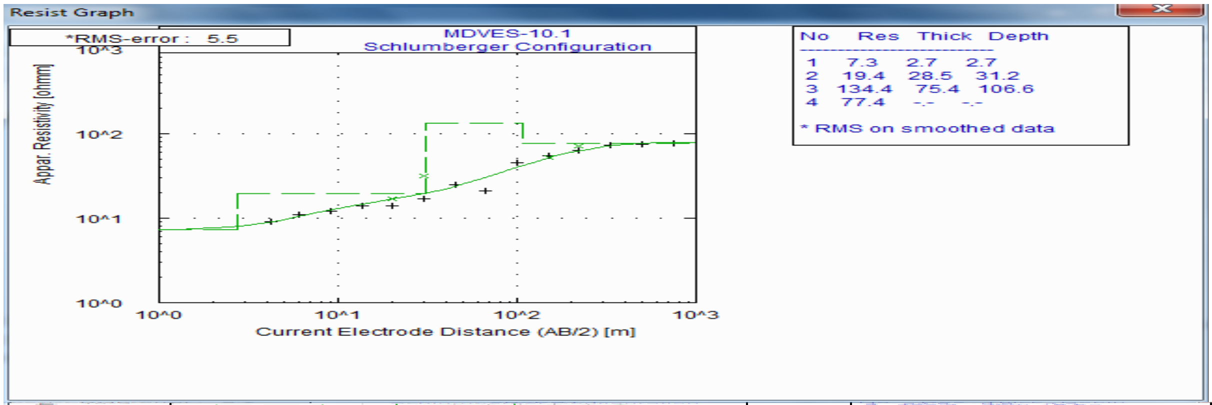
Resist Graph
*RMS-error : 5.5
MDVES-10.1
Schlumberger Configuration
Appar. Resistivity [ohmm]
Current Electrode Distance (AB/2) [m]
No Res Thick Depth
1 7.3 2.7 2.7
2 19.4 28.5 31.2
3 134.4 75.4 106.6
4 77.4 -.- -.-
* RMS on smoothed data

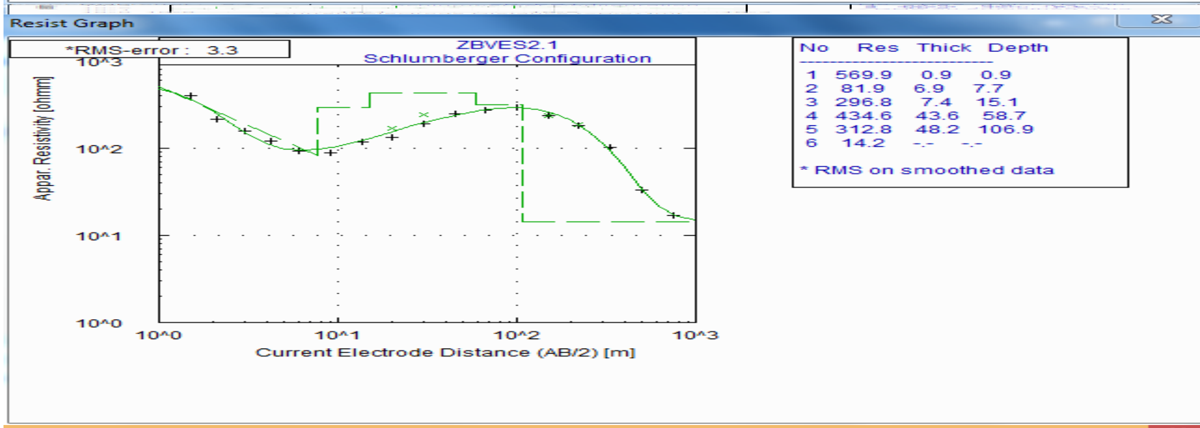
Resist Graph
*RMS-error : 3.3
ZBVES2.1
Schlumberger Configuration
Appar. Resistivity [ohmm]
Current Electrode Distance (AB/2) [m]
No Res Thick Depth
1 569.9 0.9 0.9
2 81.9 6.9 7.7
3 296.8 7.4 15.1
4 434.6 43.6 58.7
5 312.8 48.2 106.9
6 14.2 -.- -.-
* RMS on smoothed data

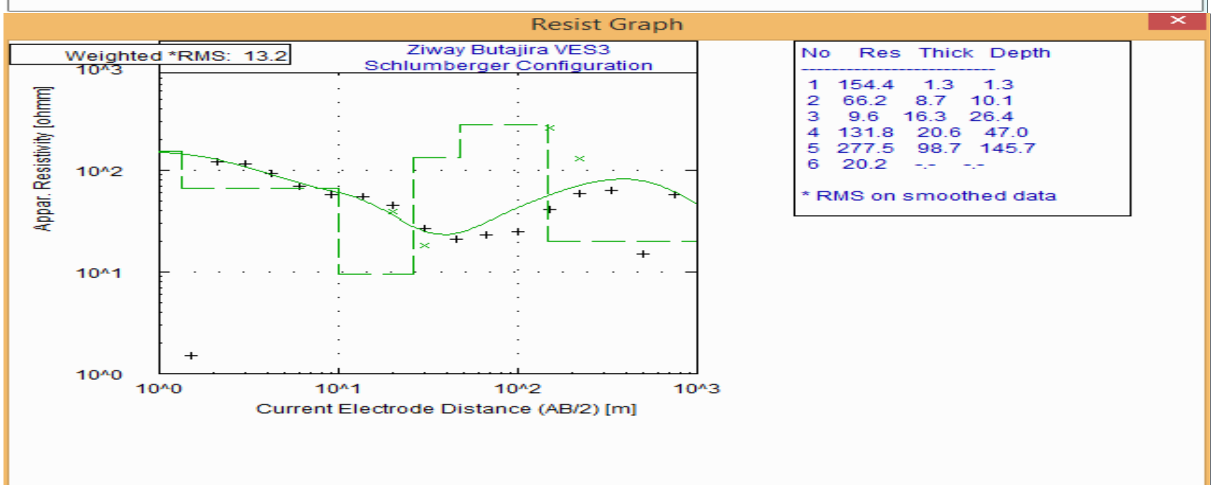
Resist Graph
Weighted *RMS: 13.2
Ziway Butajira VES3
Schlumberger Configuration
Appar. Resistivity [ohmm]
Current Electrode Distance (AB/2) [m]
No Res Thick Depth
1 154.4 1.3 1.3
2 66.2 8.7 10.1
3 9.6 16.3 26.4
4 131.8 20.6 47.0
5 277.5 98.7 145.7
6 20.2 -.- -.-
* RMS on smoothed data

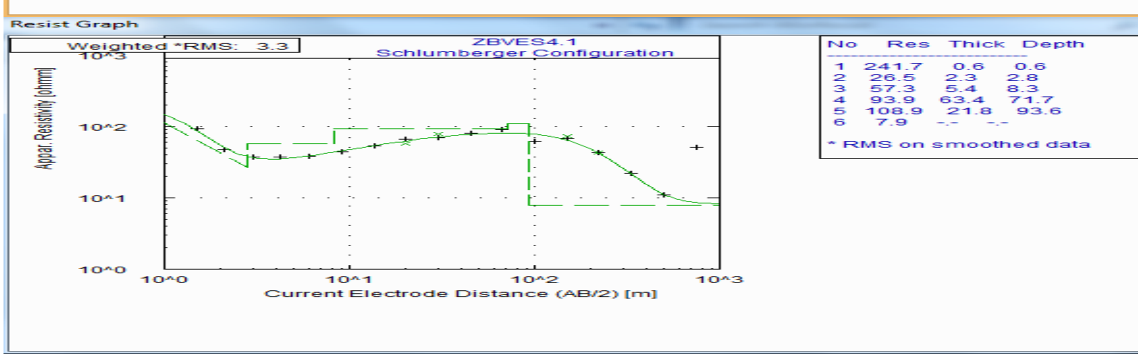
Resist Graph
Weighted *RMS: 3.3
ZBVES4.1
Schlumberger Configuration
Appar. Resistivity [ohmm]
Current Electrode Distance (AB/2) [m]
No Res Thick Depth
1 241.7 0.6 0.6
2 26.5 2.3 2.8
3 57.3 5.4 8.3
4 93.9 63.4 71.7
5 108.9 21.8 93.6
6 7.9 -.- -.-
* RMS on smoothed data

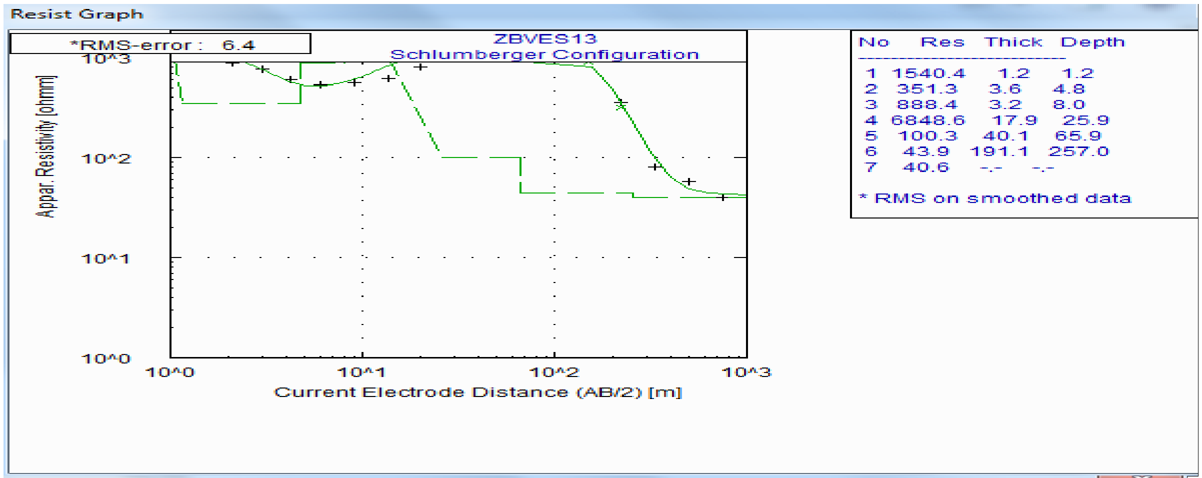
Resist Graph
*RMS-error : 6.4
ZBVES13
Schlumberger Configuration
Appar. Resistivity [ohmm]
10^3
10^2
10^1
10^0
10^0
10^1
10^2
10^3
Current Electrode Distance (AB/2) [m]
No Res Thick Depth
1 1540.4 1.2 1.2
2 351.3 3.6 4.8
3 888.4 3.2 8.0
4 6848.6 17.9 25.9
5 100.3 40.1 65.9
6 43.9 191.1 257.0
7 40.6 -.- -.-
* RMS on smoothed data

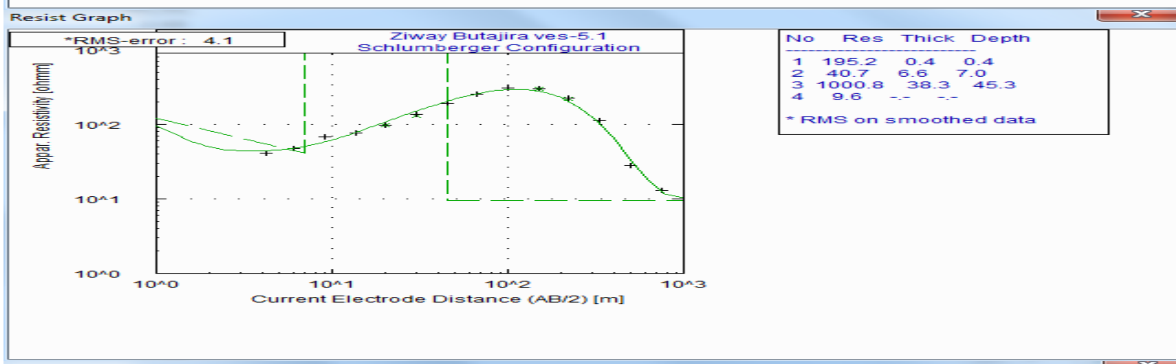
Resist Graph
*RMS-error : 4.1
Ziway Butajira ves-5.1
Schlumberger Configuration
Appar. Resistivity [ohmm]
10^3
10^2
10^1
10^0
10^0
10^1
10^2
10^3
Current Electrode Distance (AB/2) [m]
No Res Thick Depth
1 195.2 0.4 0.4
2 40.7 6.6 7.0
3 1000.8 38.3 45.3
4 9.6 -.- -.-
* RMS on smoothed data

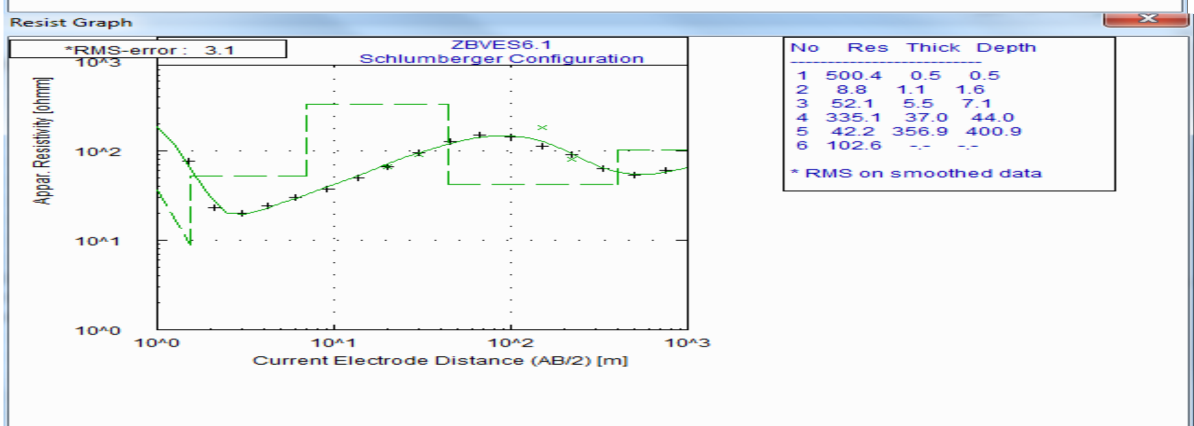
Resist Graph
*RMS-error : 3.1
ZBVES6.1
Schlumberger Configuration
Appar. Resistivity [ohmm]
10^3
10^2
10^1
10^0
10^0
10^1
10^2
10^3
Current Electrode Distance (AB/2) [m]
No Res Thick Depth
1 500.4 0.5 0.5
2 8.8 1.1 1.6
3 52.1 5.5 7.1
4 335.1 37.0 44.0
5 42.2 356.9 400.9
6 102.6 -.- -.-
* RMS on smoothed data

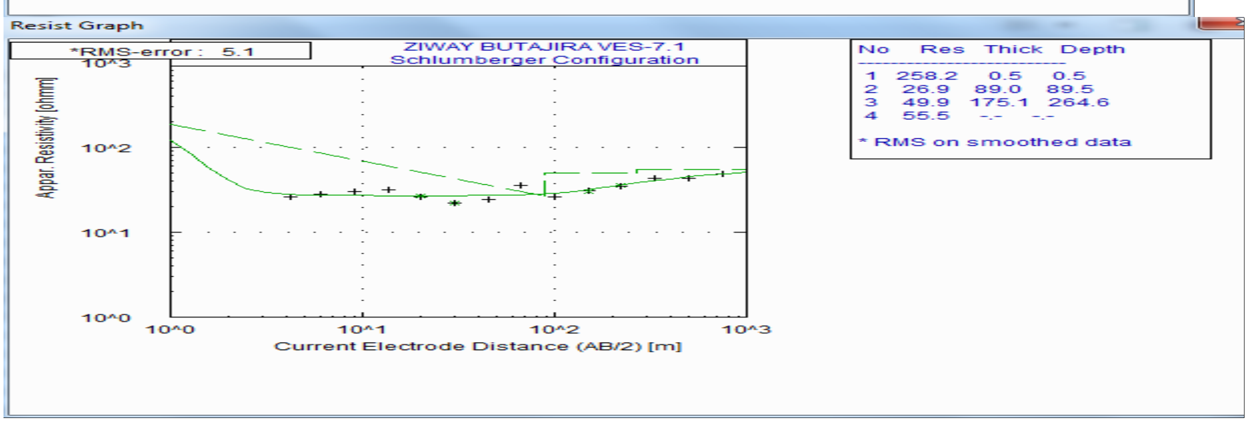
Resist Graph
*RMS-error : 5.1
ZIWAY BUTAJIRA VES-7.1
Schlumberger Configuration
Appar. Resistivity [ohmm]
10^3
10^2
10^1
10^0
10^0
10^1
10^2
10^3
Current Electrode Distance (AB/2) [m]
No Res Thick Depth
1 258.2 0.5 0.5
2 26.9 89.0 89.5
3 49.9 175.1 264.6
4 55.5 -.- -.-
* RMS on smoothed data

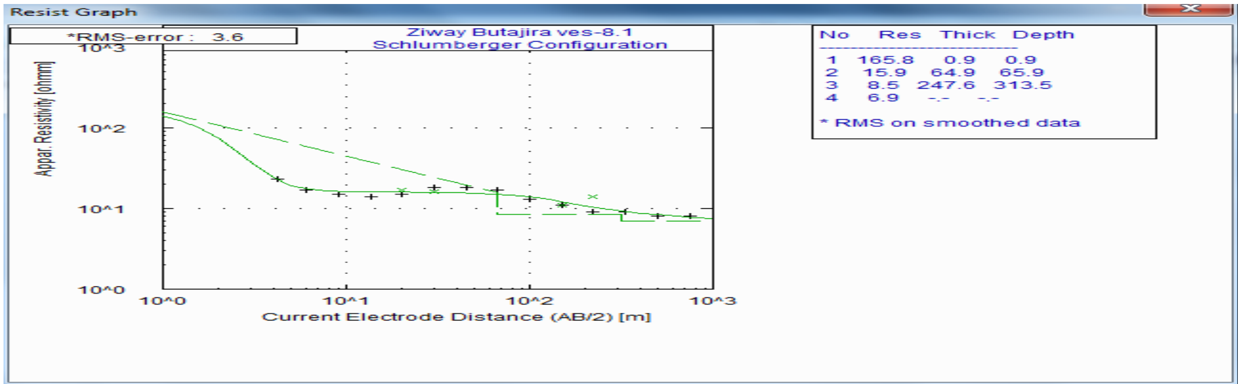
Resist Graph
*RMS-error : 3.6
Ziway Butajira ves-8.1
Schlumberger Configuration
Appar. Resistivity [ohmm]
10^3
10^2
10^1
10^0
10^0 10^1 10^2 10^3
Current Electrode Distance (AB/2) [m]
No Res Thick Depth
1 165.8 0.9 0.9
2 15.9 64.9 65.9
3 8.5 247.6 313.5
4 6.9 -.- -.-
* RMS on smoothed data

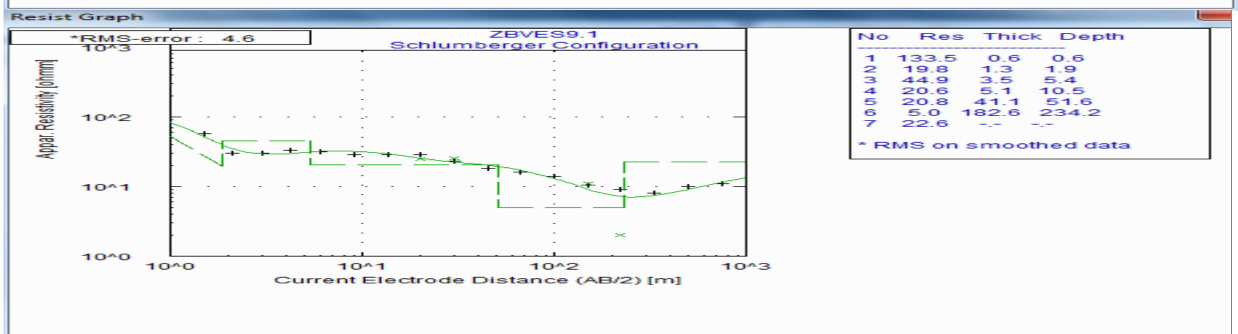
Resist Graph
*RMS-error : 4.6
ZBVES9.1
Schlumberger Configuration
Appar. Resistivity [ohmm]
10^3
10^2
10^1
10^0
10^0 10^1 10^2 10^3
Current Electrode Distance (AB/2) [m]
No Res Thick Depth
1 133.5 0.6 0.6
2 19.8 1.3 1.9
3 44.9 3.5 5.4
4 20.6 5.1 10.5
5 20.8 41.1 51.6
6 5.0 182.6 234.2
7 22.6 -.- -.-
* RMS on smoothed data

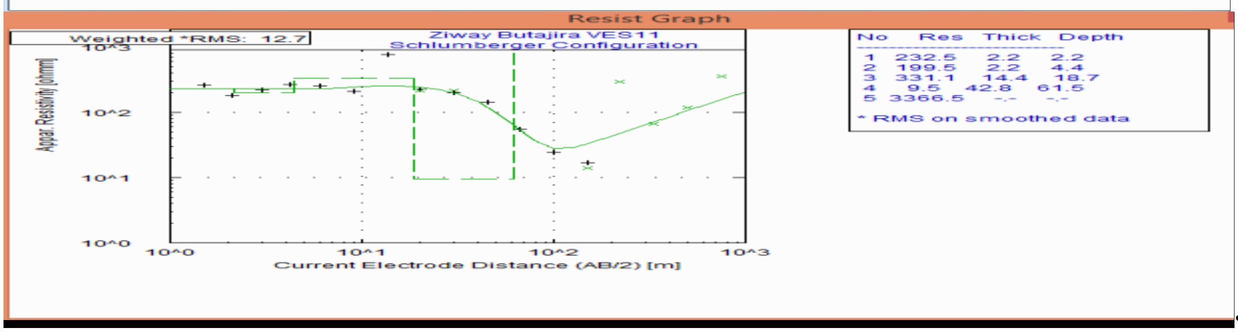
Resist Graph
Weighted *RMS: 12.7
Ziway Butajira VES11
Schlumberger Configuration
Appar. Resistivity [ohmm]
10^3
10^2
10^1
10^0
10^0 10^1 10^2 10^3
Current Electrode Distance (AB/2) [m]
No Res Thick Depth
1 232.5 2.2 2.2
2 199.5 2.2 4.4
3 331.1 14.4 18.7
4 9.5 42.8 61.5
5 3366.5 -.- -.-
* RMS on smoothed data

4

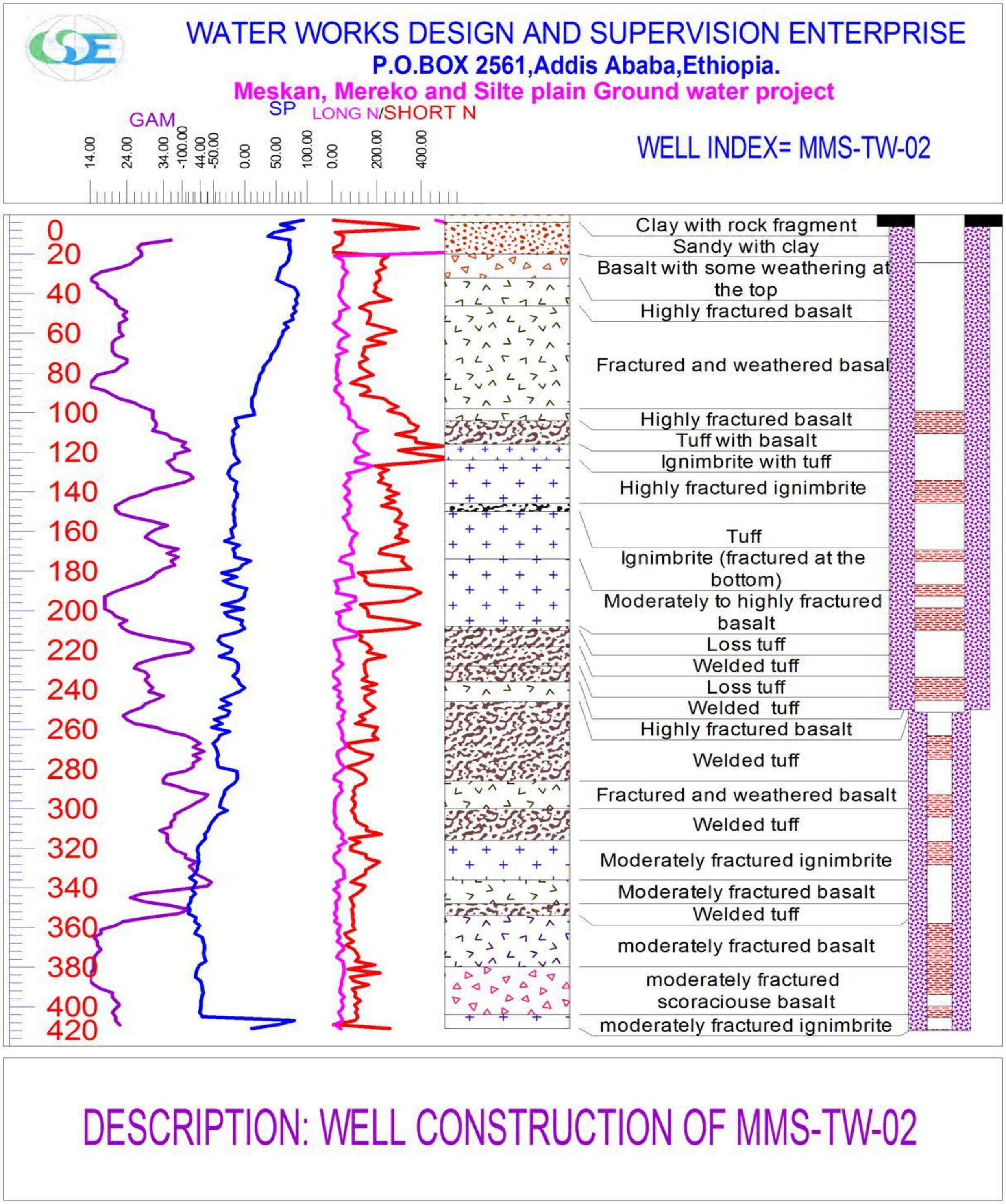

Table 1 wellog report around Butajira(VES7 to VES13) adopted from WWDES 2005

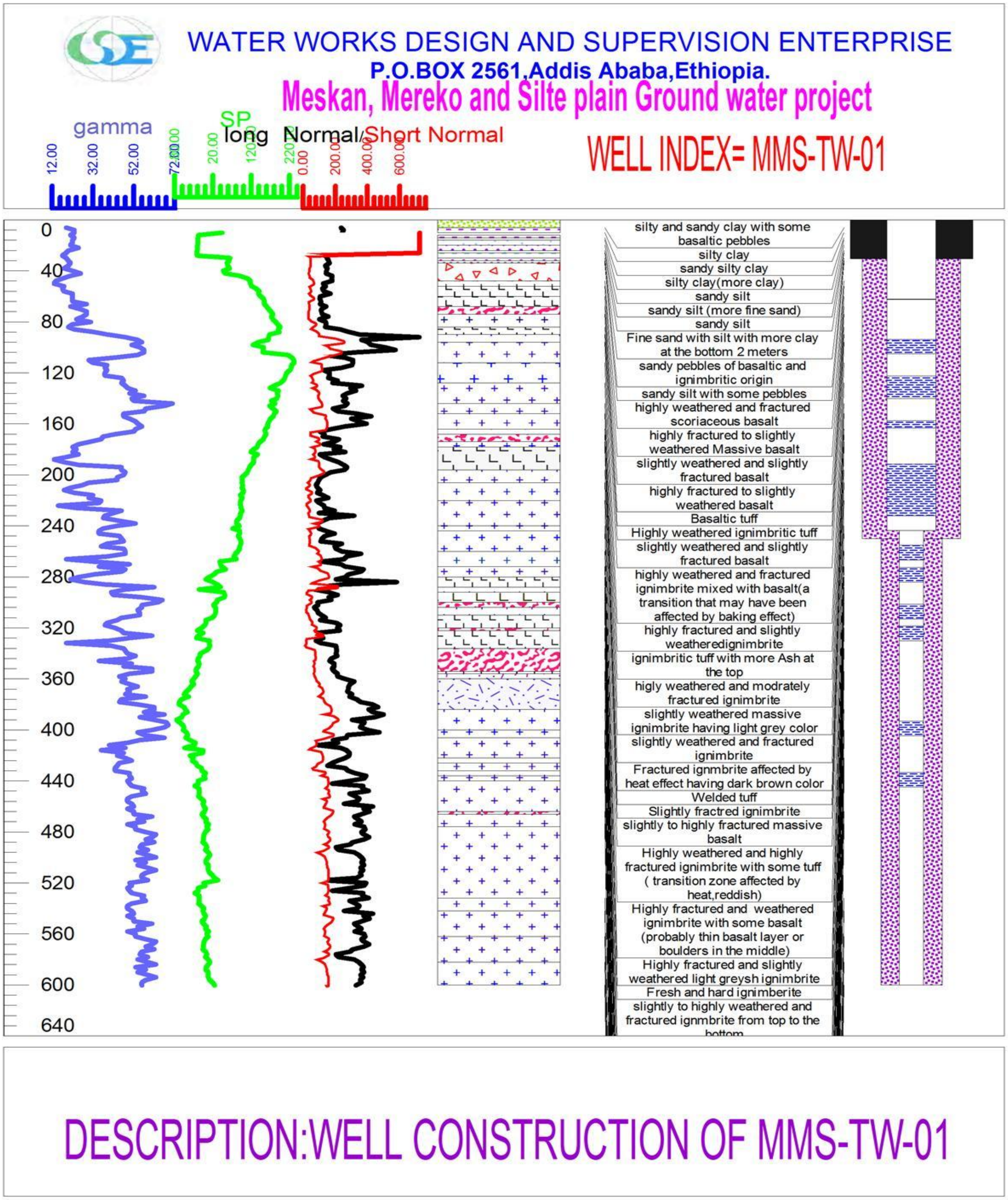

Table 2.wel log report around koshe(VES1 to VES6) adopted from WWDES2005

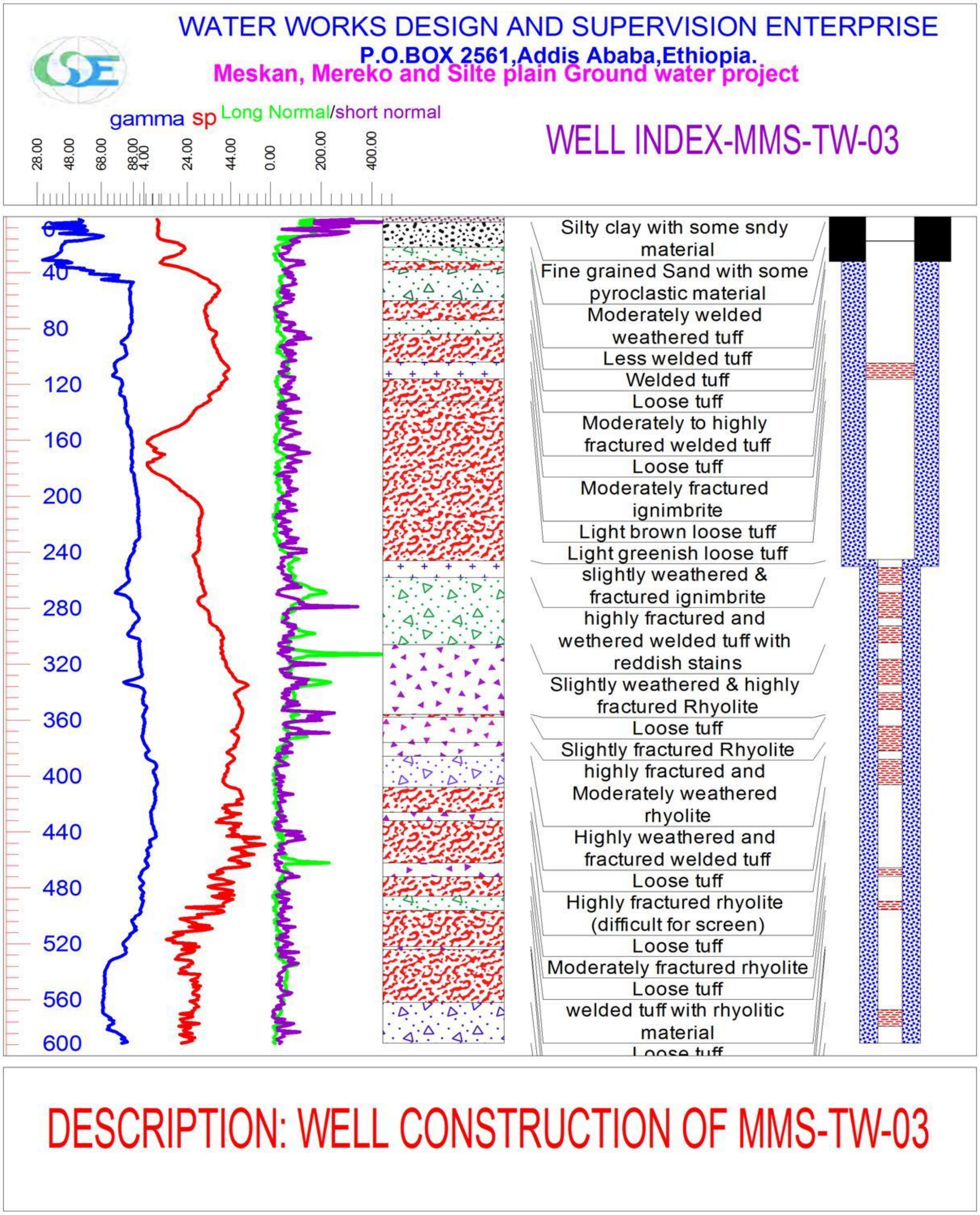

Table 3. Wellog report around miderkebd(VES6 to VES10) adopted from WWDSE2005